



6-1984

Performance of a Ground-Coupled Heat Pump during a Cooling Season

Steven D. Wix
University of Tennessee - Knoxville

Follow this and additional works at: https://trace.tennessee.edu/utk_gradthes



Part of the [Mechanical Engineering Commons](#)

Recommended Citation

Wix, Steven D., "Performance of a Ground-Coupled Heat Pump during a Cooling Season. " Master's Thesis, University of Tennessee, 1984.
https://trace.tennessee.edu/utk_gradthes/3214

This Thesis is brought to you for free and open access by the Graduate School at TRACE: Tennessee Research and Creative Exchange. It has been accepted for inclusion in Masters Theses by an authorized administrator of TRACE: Tennessee Research and Creative Exchange. For more information, please contact trace@utk.edu.

To the Graduate Council:

I am submitting herewith a thesis written by Steven D. Wix entitled "Performance of a Ground-Coupled Heat Pump during a Cooling Season." I have examined the final electronic copy of this thesis for form and content and recommend that it be accepted in partial fulfillment of the requirements for the degree of Master of Science, with a major in Mechanical Engineering.

W.S. Johnson, Major Professor

We have read this thesis and recommend its acceptance:

J.R. Parsons, Rao V. Arimilli

Accepted for the Council:

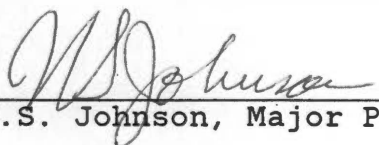
Carolyn R. Hodges

Vice Provost and Dean of the Graduate School

(Original signatures are on file with official student records.)

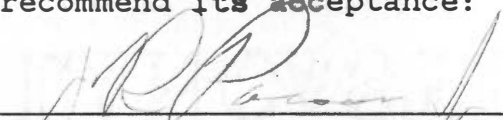
To the Graduate Council:

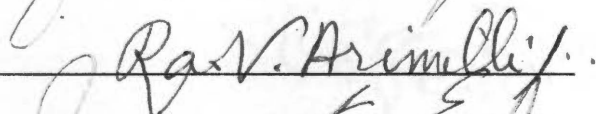
I am submitting herewith a thesis written by Steven D. Wix entitled "Performance of a Ground-Coupled Heat Pump during a Cooling Season." I have examined the final copy of this thesis for form and content and recommend that it be accepted in partial fulfillment of the requirements for the degree of Master of Science, with a major in Mechanical Engineering.



W.S. Johnson, Major Professor

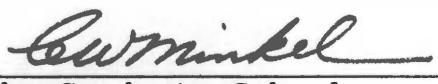
We have read this thesis and recommend its acceptance:







Accepted for the Council:



The Graduate School

1

PERFORMANCE OF A GROUND-COUPLED HEAT PUMP
DURING A COOLING SEASON

A Thesis

Presented for the

Master of Science

Degree

The University of Tennessee, Knoxville

Steven D. Wix

June 1984

ABSTRACT

A ground-coupled heat pump system was installed in TECH House I at the Tennessee Energy Conservation in Housing site located on the University of Tennessee campus. The performance of the heat pump system was evaluated for the cooling season of 1983. Data on system energy flows, power consumption, house temperatures, soil temperatures and weather conditions were gathered on an hourly basis for the entire cooling season. Weekly coefficients of performance, soil thermal conductivitys, and a seasonal performance factor were calculated from experimental data.

The performance was found to be poor when compared to a conventional air-to-air heat pump system. The seasonal performance factor for the ground-coupled heat pump system was 1.11 while typical conventional heat pump system seasonal performance factors for the Knoxville area are around 2.3. A trend of performance deterioration over the season due in part to decreasing soil thermal conductivity was found. The decreasing soil thermal conductivity was caused by a decrease in soil moisture.

The ground-coupled heat pump system was modeled using the TRNSYS and GROCS computer programs. Comparison with experimental data validated the computer model. The difference between the predicted and experimental seasonal performance factors was approximately 3 percent.

Parametric studies were performed to determine system performance under various conditions. Factors varied include soil moisture content, density, cooling load per unit coil length and far-field soil temperatures.

The predictions show that the ground-coupled heat pump should give best performance in coarse grained, well packed, moisture saturated soil. Worst performance was predicted to occur in fine grained, loose packed, dry soil.

The model was also used to predict the maximum performance of a well designed ground-coupled heat pump in the Knoxville area. The maximum predicted seasonal performance factor was 2.04.

TABLE OF CONTENTS

CHAPTER	PAGE
1. INTRODUCTION.	1
The Heat Pump	1
Types of Heat Pumps	3
Past and Current Research	9
Project Objectives.	11
2. SOIL PROPERTIES	12
Soil Relationships.	13
Soil Texture Classification	14
Soil Thermal Properties	15
Heat and Mass Transfer.	19
Soil Thermal Stability.	21
3. THE HEAT PUMP SYSTEM AND INSTRUMENTATION.	23
The Heat Pump System.	23
Instrumentation	25
4. EXPERIMENTAL RESULTS.	37
Heat Pump Performance Data.	37
Experimental Thermal Conductivity	43
Soil Moisture Measurements.	51
Soil Observations	55
Soil Thermal Stability.	57

CHAPTER	PAGE
5. MODEL COMPONENTS AND RESULTS.	59
Model Description	59
Model Verification.	66
Parametric Studies.	72
6. CONCLUSIONS AND RECOMMENDATIONS	82
LIST OF REFERENCES	87
APPENDICIES.	93
APPENDIX A.	94
APPENDIX B.	97
APPENDIX C.	98
APPENDIX D.	100
APPENDIX E.	101
APPENDIX F.	106
VITA	109

LIST OF FIGURES

FIGURE	PAGE
1-1. Heat Pump Schematic	2
1-2. System Performance Deterioration.	5
3-1. Plan View of Horizontal Ground Coil	26
3-2. Location of Ground Temperature Probes	31
3-3. Location of Ceramic Soil Moisture Meters.	33
4-1. Weekly Cooling COPs	41
4-2. Hourly Soil Temperature 15.2 Centimeters from Coil	46
4-3. Weekly Soil Thermal Conductivity.	50
4-4. Soil Moisture Data.	52
4-5. July 1983 Time Average Moisture Profile	54
5-1. GROCS Node Configuration.	64
5-2. Coil Inlet Temperature Comparison	67
5-3. Coil Outlet Temperature Comparison.	68
5-4. Energy to Ground Comparison	70
5-5. Heat Pump Power Comparison.	71
5-6. Moisture Effects on SPF	74
5-7. Density Effects on SPF	76
5-8. Cooling Load Effect on SPF.	78
5-9. Coil Outlet Temperature vs Cooling Load	79

FIGURE	PAGE
C-1. Moisture Meter Calibration Curve.	99
E-1. Temperature vs Cooling Capacity102
E-2. Temperature vs Energy to Ground103
E-3. Temperature vs Heat Pump Power.104
E-4. Temperature vs COP.105

CHAPTER 1

INTRODUCTION

The history of heat pumps began in 1850 when, in Appalachicola, Florida, John Gorrie invented the first ice making device. Gorrie built a steam engine that moved a piston which compressed air. The air was allowed to expand quickly and this expansion caused the air temperature to drop below the freezing point of water. Gorrie used ice produced from his device to cool malaria patients in an attempt to cure the patients of their illness.

Lord Kelvin was also another pioneer in developing the heat pump. In 1850, Lord Kelvin presented to the Royal Society his theory of a "heat multiplier" device. Kelvin's "heat multiplier" theory and Gorrie's ice making device are the basis for the modern heat pump(1).

The Heat Pump

The basic components of a heat pump are a compressor, an evaporator, a condenser and an expansion valve. Figure 1-1 illustrates a basic heat pump system. The compressor takes low pressure vapor at

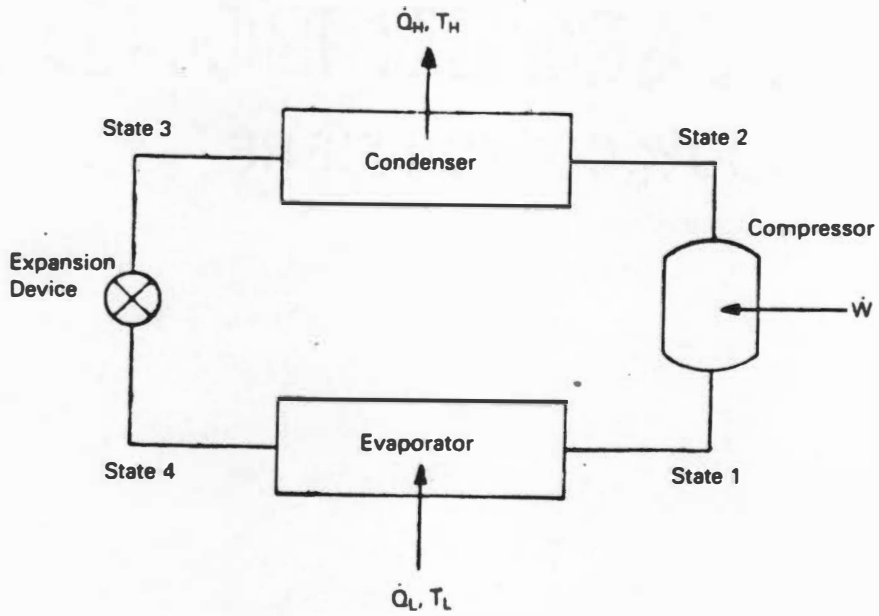


Figure 1-1. Heat Pump Schematic

State 1 and compresses the vapor to a high pressure, State 2. The high pressure vapor then passes through the condenser where the vapor releases energy and changes phase. At State 3, the fluid is a high pressure liquid. The liquid then passes through the expansion valve and enters the evaporator at State 4 as a low pressure mixture of liquid and vapor. As the mixture passes through the evaporator, energy is added. The result is a low pressure vapor at State 1.

Types of Heat Pumps

The types of heat pumps in use today are air-to-air, air-to-water, earth-to-air, earth-to-water, water-to-air, and water-to-water(2). Each type refers to the heat source (sink) to heat sink (source) heat transfer for heating (cooling). The air-to-air heat pump is the most common type of heat pump in use today for residential applications. The use of air as the heat transfer fluid allows great flexibility in the design of heating and air conditioning systems. Air-to-air heat pumps also are usually manufactured in modularized compact packages which contain the heat pump components. The packaging allows the heat pump to be mass-produced thus reducing the price to the consumer.

Air-to-water heat pumps use water as the heat transfer fluid in moving energy into or out of the conditioned space. The air-to-water heat pumps have frequent application in large buildings where zone control is necessary(2). The primary disadvantage of the air to air and air to water heat pumps is that the performance deteriorates significantly when the systems are needed the most. Figure 1-2 illustrates the system performance deterioration(3). During the heating season, frost may form on the outside air coil. Some sort of defrost cycle is used to stop the coil frosting but adds to the operating costs and requires an auxiliary heater.

Earth-to-air and earth-to-water heat pumps use the earth as a heat sink or source. These heat pumps use direct evaporation or condensation of the refrigerant in the ground coil. Earth-to-air and earth-to-water heat pumps do not experience the temperature fluctuations that heat pumps using air as the outdoor heat sink or source encounter since the earth is a temperature moderator. Since the range of annual temperature fluctuations is less for earth-to-air and earth-to-water heat pumps, the heat pump system performance should not deteriorate as significantly as air type heat pumps. The installation costs, however,

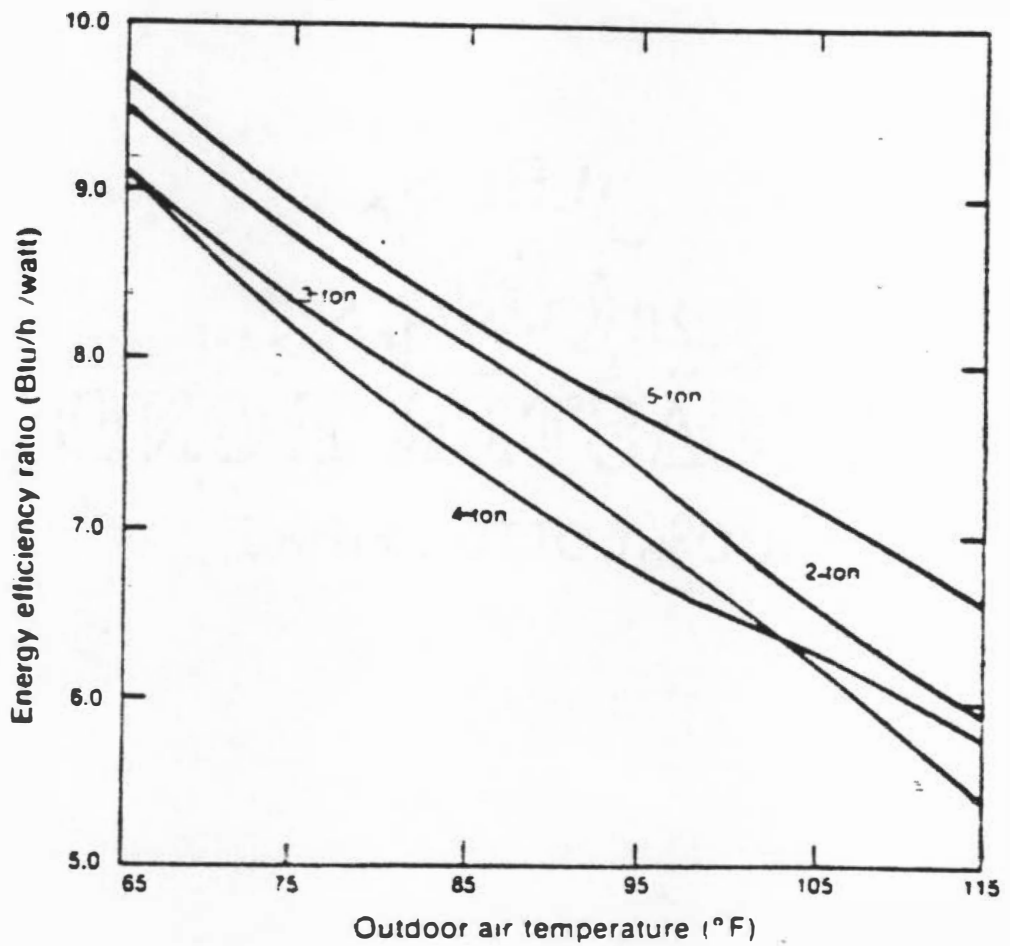


Figure 1-2. System Performance Deterioration

are much higher than air type heat pumps. The cost of high pressure tubing and the large volume of refrigerant needed for the ground coil would further increase initial costs(2).

Water-to-air and water-to-water heat pumps use ground water, air or the earth as the outside heat sink or heat source. When ground water is used, at least one well is needed since streams or lakes are not usually available. Ground water is not practical unless there is some way to return the water to the underground reservoir. Any general widespread use of ground water without returning the water to the underground reservoir would result in depletion of this valuable resource and would not be in the public interest.

One method of returning ground water to the underground reservoir is a dual well system where one well is used to extract water and a second well is used to return the water to the underground reservoir. The practicality of a dual well system depends upon local conditions, well spacing, local codes, environmental considerations, etc. This recycling scheme may be economically justifiable and practical where there are shallow, thick water sands(4).

The chief advantage of using ground water instead of air for the outdoor heat sink or source is that ground water is at nearly constant and relatively high temperature in the winter and low temperature in the summer when compared to the air temperature(2). By having a nearly constant outdoor sink or source temperature, it is possible to design a unit that operates at maximum efficiency for a particular range of ground temperatures. This would result in reduced operating costs.

Some other disadvantages in the use of ground water in heat pump applications are corrosion and scaling problems on the heat transfer surface and higher installation costs when compared to air type heat pumps. The water composition, location and temperature is usually unknown until after the well has been drilled. There is also the possibility that the well could dry up(2).

There are two basic types of water-to-air and water-to-water heat pumps that use the earth as a heat sink or source. The types are the vertical coil and horizontal coil heat pump systems. Both systems can be used in areas with limited water availability and/or corrosive minerals in the water supply. The vertical

earth coil system is composed of a well or series of wells with a u-shaped heat exchanger in each well. The vertical coil heat exchanger installation cost is \$21.33 (1979 dollars) per meter as reported by Bose at Oklahoma State University(5). Bose also mentions that a minimum length ratio of 30.5 meters of wetted coil per ton of summer cooling is recommended for a vertical coil heat exchanger in the Oklahoma area.

The horizontal coil heat pump system is the subject of this study. A horizontal coil heat pump utilizes an underground piping network as a heat exchanger. Some fluid other than the heat pump refrigerant, such as water, is used as the heat transfer fluid. The installation cost of a horizontal coil heat exchanger, also reported by Bose, is \$5.75 (1981 dollars) per meter(5). Bose suggests a length ratio of between 91 and 106 meters per ton of summer cooling for a horizontal coil heat exchanger. Bose suggested length ratio places the cost per ton between \$525.00 and \$612.50 for the horizontal coil.

Several disadvantages of the horizontal coil heat pump system are the large amount of surface area required for the coil and, when used during the summer, the possibility of the soil drying in the vicinity of the coil. Such drying would reduce the thermal

conductivity of the soil which would cause a rise in the coil fluid temperature. This increase in coil fluid temperature would cause the condenser pressure to increase, thus reducing the heat pump efficiency and cause the heat pump to use more power. Circumstances could arise where the increase in condenser pressure is so great that the heat pump high pressure sensor would cause the heat pump to stop operating.

Past and Current Research

Much research was conducted in the 1940's and 1950's on ground-coupled heat pumps. A survey report on current research as of 1953 was presented in the Edison Electric Institute Bulletin(6). Listed were 28 research projects in progress or completed. Twenty two of the projects involved actual heat pump installations. Nine of the projects dealt with heating only, three were cooling only and the remaining ten were heating and cooling. The installations were as far north as Connecticut, as far south as Alabama and as far west as Washington. The heat transfer rates reported range between 1.10 and 6.44 W/m-C for heating and between 0.74 and 2.38 W/m-C for cooling. Seasonal performance data were not given.

By the late 1950's, interest in ground-coupled heat pumps waned due to cheap and abundant electricity. Interest has been restored lately due to the energy crises of 1973 and 1978.

As of 1980, over 1000 heat only heat pumps have been installed in Sweden(7). Depending upon the capacity, the total installed system cost is between \$7300 and \$8400. AGA Thermia is the installer and accepts orders only where moist clay is present.

There have been over 100 ground-coupled heat pumps installed in the Stillwater, Oklahoma area(5). The earth coils are buried at a 1.22 meter depth and use between 61 and 91 meters of coil per ton of heat pump capacity.

There has been some research recently into increasing ground-coupled heat pump performance, particularly for heating. Cooling data is sketchy at best. Bose (5) found system performance deterioration at the beginning of the cooling season and a leveling of performance throughout the middle and end of the cooling season. Metz (8) has developed a computer program called GROCS which models ground heat transfer. GROCS has been applied to ground-coupled heat pump systems and validation of the program is currently underway(9,10).

Project Objectives

The first objective of this study is to experimentally analyze the performance of a ground-coupled heat pump during a cooling season in the Tennessee valley region. Specifically, the cooling seasonal performance factor of the heat pump system has been determined. The effects of soil properties on performance are evaluated. A detailed description of the ground-coupled heat pump and instrumentation is presented in Chapter 3. Experimental results are presented in Chapter 4.

The second objective of this study is to develop and verify a computer model of a horizontal coil ground-coupled heat pump. The model of the ground-coupled heat pump system was developed using the existing programs TRNSYS (11) and GROCS(8). The model of the ground-coupled heat pump is presented in Chapter 5. Parametric studies using the model were performed and the results are presented in Chapter 5. The model was used to predict the effects soil properties have on ground-coupled heat pump performance and a maximum limit of performance for the Knoxville region.

CHAPTER 2

SOIL PROPERTIES

A ground-coupled heat pump must operate with a higher system efficiency than an air to air heat pump in order to justify the higher initial cost of the ground-coupled heat pump. This implies that large amounts of heat must be transferred to the soil during the cooling season in an efficient manner. Since the physical and thermal properties of soil play an important role in the aforementioned transfer of heat, a discussion of soil physical and thermal properties seems appropriate.

Soil is a nonhomogeneous material that is usually subdivided into three phases, solid, liquid, and gas. The solid phase can consist of crystalline and/or noncrystalline particles of various shapes and sizes. A percentage of the solid material can be organic material. The solid phase can be thought of as a matrix which forms the framework of the soil. The manner in which the soil particles form the soil matrix also form the void spaces which contain the liquid and gas phases(12).

The liquid phase is a water solution containing dissolved gases, soluble salts and organic and inorganic solutes(12). The gaseous phase is similar to the atmosphere but differs in the proportion of the components(12). The gas phase is usually assumed to be air. The three-phase system is a simple way to express commonly used soil properties such as water content, porosity and void ratio.

Soil Relationships

Volume and mass relationships among the three phases in the soil and some basic parameters useful in characterizing soils will now be considered. The volume relationships of each phase can be expressed by,

$$V_s + V_g + V_l = 1 \quad (2-1)$$

where,

V_s, V_g, V_l = volumetric fractions of the
solid, gas and liquid
phases, respectively.

Porosity is a measure of the void space in the soil. Porosity is usually in the range of 30 to 60 percent. Course grained soils such as sand tend to have porosities between 30 and 40 percent and fine

textured soils such as clay have porosities between 40 and 60 percent(13). Porosity is defined as the ratio of the volume of the void space to the sum of the volumes of the void space and solid material in the soil, or,

$$P=V_v/V \quad (2-2)$$

where,

$$V_v=V_g+V_l$$

Water content is usually defined on a percent basis as the mass of the moisture to the mass of the solid, or,

$$WC=W_w/W_d*100 \quad (2-3)$$

where,

W_m =weight of the moisture

W_d =weight of dry soil.

Soil Texture Classification

Two soil classification systems based on particle size are in use today. These systems have been developed by the United States Department of Agriculture(14,15) and by Atterberg(13).

A rough field test can be performed to determine soil texture. With wet soil, the feel of the soil can be determined between the thumb and finger. Sand particles have a gritty feel, silt has a smooth or floury feel and clay is plastic or sticky(13).

Soil Thermal Properties

Thermal conductivity, volumetric heat capacity, and thermal diffusivity are thermal properties that can affect the performance of a ground-coupled heat pump. Volumetric heat capacity is a relatively simple property to determine, given the volumetric fractions of the individual soil components. DeVries(16) presented an equation to determine the volumetric heat capacity,

$$C=V_s*C_s+V_l*C_l+V_g*C_g \quad (2-4)$$

where,

C_s, C_l, C_g = Heat capacity of the solid, liquid
and gas components of the soil,
respectively.

DeVries(16) also developed an empirical equation for calculating the volumetric heat capacity. The heat capacity of the gas phase is neglected since the gas

phase contributes very little to the overall volumetric heat capacity(16). DeVries used data gathered by other researchers (17,18,19,20) to determine the volumetric heat capacity of the soil solid phase. The equation developed by DeVries, per unit volume, is

$$C=0.46*V_m+0.6*V_o+V_w \text{ cal cm}^{-3} \text{ C}^{-1} \quad (2-5)$$

where,

V_m, V_o, V_w =volume fraction of the solid

minerals, solid organic material

and the liquid phase where water

is assumed to be the only component,

respectively.

Determining soil thermal conductivity is much more difficult than determining soil volumetric heat capacity. Many experimental values for various types of soils have been presented in the literature(13,21,22,23). The experimental values should be used only if the soil in question is similar in not only texture and mineral composition but also moisture content and density. For example, Kersten (21) reports that, for Dakota sandy loam, as the soil moisture content is increased from 1.9 percent to 4.9 percent, the soil thermal conductivity increased by

more than a factor of 9, from 0.24 to 1.96 W/m-C. As for the influence of density, Hartly and Black (24) report that, at moisture contents below 5.0 percent by weight, a change in density from 1280 to 1440 kg/m³ can cause the thermal conductivity to increase by more than a factor of 2.

The soil thermal conductivity cannot be calculated based entirely on the thermal properties of the components of the soil in question. Mass transfer must also be included which leads to the concept of an "apparent" thermal conductivity which would include mass transfer effects. A method for determining the apparent soil thermal conductivity has been presented by DeVries(16) and was derived from an equation by Maxwell and Rayleigh for calculating the electrical conductivity of porous material.

The apparent thermal conductivity of a multiphase porous material is given by,

$$K_{ap} = \frac{V_w K_w + W_{Fa} K_a V_a + \sum_{i=1}^N W_{Fi} K_i V_i}{V_w + W_{Fa} V_a + \sum_{i=1}^N W_{Fi} V_i} \quad (2-6)$$

where,

V_w, V_a, V_i = volumetric fraction of water, air and individual soil components, respectively, and

K_w, K_a, K_i = thermal conductivity of water, air
and individual soil components,
respectively, and,

W_{Fi}, W_{Fa} = weighing factors,

N = number of types of soil particles.

The weighing factors, W_{Fi} and W_{Fa} , have a physical meaning in that they represent the ratio of the temperature gradient across the soil particles or air to the temperature gradient across the water(16). The individual values of the weighing factors are dependent upon the size, shape and relative position of the solid soil particles and can be calculated by making assumptions of the size and shape of the solid particles(16). Several researchers (22,25) have used this theory with good success.

Thermal diffusivity is the ratio of thermal conductance to heat capacity and can be easily calculated once the thermal conductivity and heat capacity are known. Lunardini(25), using data obtained by Kersten (21) has presented graphs of apparent thermal conductivity, heat capacity and thermal diffusivity as a function of moisture content and density for both coarse and fine grained soils. Lunardini(25) shows that, for fine grained soils such

as the soil at the TECH site, the thermal diffusivity has a weak dependence on changes in moisture content except when the moisture content is low. Course grained soils show a steady increase in thermal diffusivity as the moisture content increases.

Heat And Mass Transfer

The transport of heat and mass in porous materials is a complex problem and not readily solved. Heat transfer in moist soil is complicated by the fact that moisture movement is induced by temperature gradients. The moisture movement gives rise to sensible and latent heat transfer which influences the temperature distribution in the soil(16).

Phillip and DeVries (26) present a theory of combined heat and mass transfer through the use of two coupled differential equations with two dependent variables, temperature and moisture content. A somewhat simplified theory was developed (16) based on the assumption that heat transfer due to liquid movement is negligible. Rose (27) presents evidence to support this assumption. This theory should not be used when appreciable liquid movement is expected due to gravity and/or pressure differences. By neglecting

liquid water migration, soil heat transfer can be described by heat conduction and latent heat transfer due to vapor migration(16).

Vapor pressure gradients, caused by temperature gradients, are the driving potential of the vapor migration. The vapor migration occurs in the gas-filled pores of the soil. According to DeVries(16), the vapor flux due to temperature gradients is approximately proportional to the temperature gradient across the gas-filled pores and can be described mathematically as an increase in the heat conduction in the pore. Therefore, the apparent thermal conductivity of the gas-filled pore is composed of a normal heat conduction term and a vapor transport term, or,

$$K_p = K_a + K_v \quad (2-7)$$

where,

K_a , K_v =air thermal conductivity and vapor transport contribution, respectively.

DeVries uses the apparent thermal conductivity of the gas-filled pore as the thermal conductivity of the air phase of the soil in order to calculate the overall apparent soil thermal conductivity.

Sepaskahah and Boersma (28) have shown that for certain types of soils, at elevated temperatures, the calculated apparent soil thermal conductivities are lower than experimental soil thermal conductivities. Hadas (29) proposes that turbulence in the air pores is a possible cause for this discrepancy and suggests that the simplified theory be modified to account for higher rates of vapor diffusion due to turbulence. A "mass enhancement factor" should be multiplied to the vapor transport contribution term of the apparent thermal conductivity equation. Hadas reports that the mass enhancement factor is between 1 and 5. However, other researchers(27,30) have reported values of between 1 and 129.

Soil Thermal Stability

Hartly and Black (24) report that soil drying next to a cylindrical heat source occurs in two distinct stages. During the first stage, termed the thermally stable region, the rate of moisture migration away from the heat source decreases until a critical moisture content is reached. The second stage then occurs, known as the thermally unstable region, and is marked by an increase in the rate of moisture migration until

the soil adjacent to the heat source is almost completely dry. The value of the critical moisture content is independent of the surface heat transfer rate and is a function of the initial moisture content.

(24) However, the thermal stability of the soil is a strong function of the surface heat transfer rate. Hartly and Black (24) also suggest that, for a given soil, there will be a surface heat transfer rate below which significant drying will be delayed for a considerable length of time, possibly indefinitely.

CHAPTER 3

THE HEAT PUMP SYSTEM AND INSTRUMENTATION

A ground-coupled heat pump was installed prior to the winter of 1982-83 at the Tennessee Energy Conservation in Housing (TECH) site. The TECH site is a joint venture by the University of Tennessee, the Tennessee Valley Authority, the Department of Energy through Oak Ridge National Laboratory and a consortium of private industries as a research and demonstration project in residential energy utilization techniques. The site consists of two solar houses (TECH house I and IV), a passive solar modular house (TECH house V), an annual cycle energy system (ACES) house (TECH house II) and a control house (TECH house III). The TECH site is located at the U.T. Institute of Agriculture Experiment Station, in Knoxville, Tennessee.

The Heat Pump System

TECH house I, in which the ground coupled heat pump system is installed, is a 1904 square foot passive solar home. The energy conservation features of TECH house I include external window shading devices that reduce direct solar gain during the cooling season,

water filled tubes located in the conditioned space that store direct solar gain during the heating season and more insulation than in a conventionally built home. TECH house I was occupied during the cooling season, thus providing realistic energy consumption.

The ground-coupled heat pump system used in this study consists of four main components. The components are a water-to-water heat pump, a water to air heat exchanger, a pipe buried horizontally in the ground for use as a heat exchanger, and two circulation pumps.

The heat pump used for this experiment was a TETCO water to water heating only heat pump. Cooling capacity is 2.1 tons at a condenser inlet temperature of 30.0 C. Cooling capacity was determined from experimental data. Cooling was achieved by redirecting the water-methanol brine via three way valves. The redirection of the brine allows the ground coil to act as a condenser in the summer and an evaporator in the winter.

Gorman-Rupp series 14520 pumps were used to circulate the water-methanol brine. Measured flow rates were 2.5 cubic meters per hour through the ground coil and 2.6 cubic meters per hour through the water to air coil(31). The power consumption of each pump was approximately 160 watts.

The ground coil consists of a polybutylene pipe with an inside diameter of 3.5 centimeters and a wall thickness of 0.3 centimeters. Figure 3-1 shows the location of the coil relative to TECH house I. The thermal conductivity of the polybutylene pipe is 0.2 W/m-C(32). The installed coil length is 206 meters and is buried at approximately a 1.2 meter depth. The trench in which the ground coil was placed was dug by a mechanized ditch digger. The fill dirt used in the trench was the soil excavated from the trench. There was no special preparation of the trench before the ground coil was installed. The soil in the trench was packed by running the wheel of the ditch digger along the length of the trench after the installation of the coil.

Instrumentation

The parameters measured were the energy flow between the heat pump and the ground heat exchanger, the energy flow between the heat pump and the conditioned space, electric energy consumption of the heat pump system, soil temperatures, heat pump system temperatures and soil moisture content. All variables except the soil moisture measurements were sampled by a

Hewlett-Packard data acquisition system. The soil moisture measurements were taken by hand. The data acquisition system collected data on an hourly basis. Digital signal outputs such as the energy flows and the electrical energy consumptions were summed by counters over the sample period. At the end of the sample period, the contents of the counters and the analog signal outputs such as the temperature measurements were placed on a magnetic tape for storage. The counters were then reset to zero for data summation over the following hour.

Energy flows. Two energy flow meters were used in this research effort. The meters were located in the brine loop between the heat pump and the brine to air heat exchanger and in the brine loop between the heat pump and the ground heat exchanger. A Badger model MS-E5 nutating disk flowmeter and a pair of Winsco model 2100-1-6 high accuracy platinum resistance temperature devices (PRTD) are the components used in the in-house constructed energy flow meters. The flowmeter outputs a pulse signal whose frequency is proportional to the flowrate and the PRTD's output a voltage proportional to the temperature. The

individual PRTD output voltages are subtracted electronically and converted to a frequency.

The energy flows are determined by the following expression,

$$Q = K_{cal} * F_{flow} * F_{delt} \quad (3-1)$$

where,

Q = measured energy flow,

K_{cal} = calibration data constant,

F_{flow} = flowmeter signal frequency,

F_{delt} = temperature difference signal frequency.

The calibration data constant, K_{cal} , is determined by performing an in-situ calibration of the energy flow desired. The maximum uncertainty of the ground coil energy measurements for the 1983 cooling season is 7.4 percent. For the brine to air coil energy measurement, the uncertainty is also 7.4 percent. The error in the energy flow measurements consisted of a drift in the calibration constant and an error associated with the accuracy of the instrumentation used to measure the energy flow. The drift in the calibration constant is most likely due to the change in brine fluid properties and is the major contributor to the error in the energy flow measurements. Detailed error analysis is presented in Appendix A.

Power consumption. Measurement of the individual system component power consumption was accomplished through the use of a system of watt-hour submeters. The submeters measured the purchased power of the heat pump compressor, two circulation pumps, the air handling system and the total house power consumption.

The watt-hour meters used to measure the power consumption of the heat pump, circulation pumps and air handling system are General Electric single phase, 15 amp, 240 volt, model AR-5, type I30 meters. The watt-hour meter used to measure total house power is a General Electric three phase, 240 volt, type I-60-S.

The revolutions of the eddy disk in each watt-hour meter are counted using an optical sensor and a thin painted strip on the eddy disk. The sensor detects a change in reflected light due to the painted strip and emits a pulse. These pulses are counted by the data acquisition system and electronically multiplied by the power constant of the individual meter to obtain the power reading. This method does not cause any mechanical friction in the system which could induce error in the power consumption measurement. The error in the accuracy of each submeter is 0.5 percent(33). The total measurement error, including the error in the

instrumentation used to measure each watt-hour meter is 1.0 percent.

Temperature measurement. Minco model S9298 PRTD's were used to measure ground temperatures. The location of the sensor array at the approximate midpoint of the coil is presented in Figure 3-2. The sensor attached to the coil is insulated and, therefore, is a measure of the coil wall temperature. A total of fifteen PRTD's were used to measure the soil temperature distribution in the vertical and horizontal planes. The soil surface temperature, the temperature at a three meter depth and the coil wall temperature at 25 and 75 percent of the coil length was also measured. According to the manufacturer (34), the error associated with the PRTD measurement is 1.3 percent. The total measurement error of the PRTD's and the instrumentation to measure and record data from the PRTD's is 1.8 percent.

The house indoor wet and dry bulb temperatures were measured using an Analog Devices AC 2626 temperature probe. The probe is a two-terminal integrated circuit temperature transducer which produces an output current linearly proportional to the

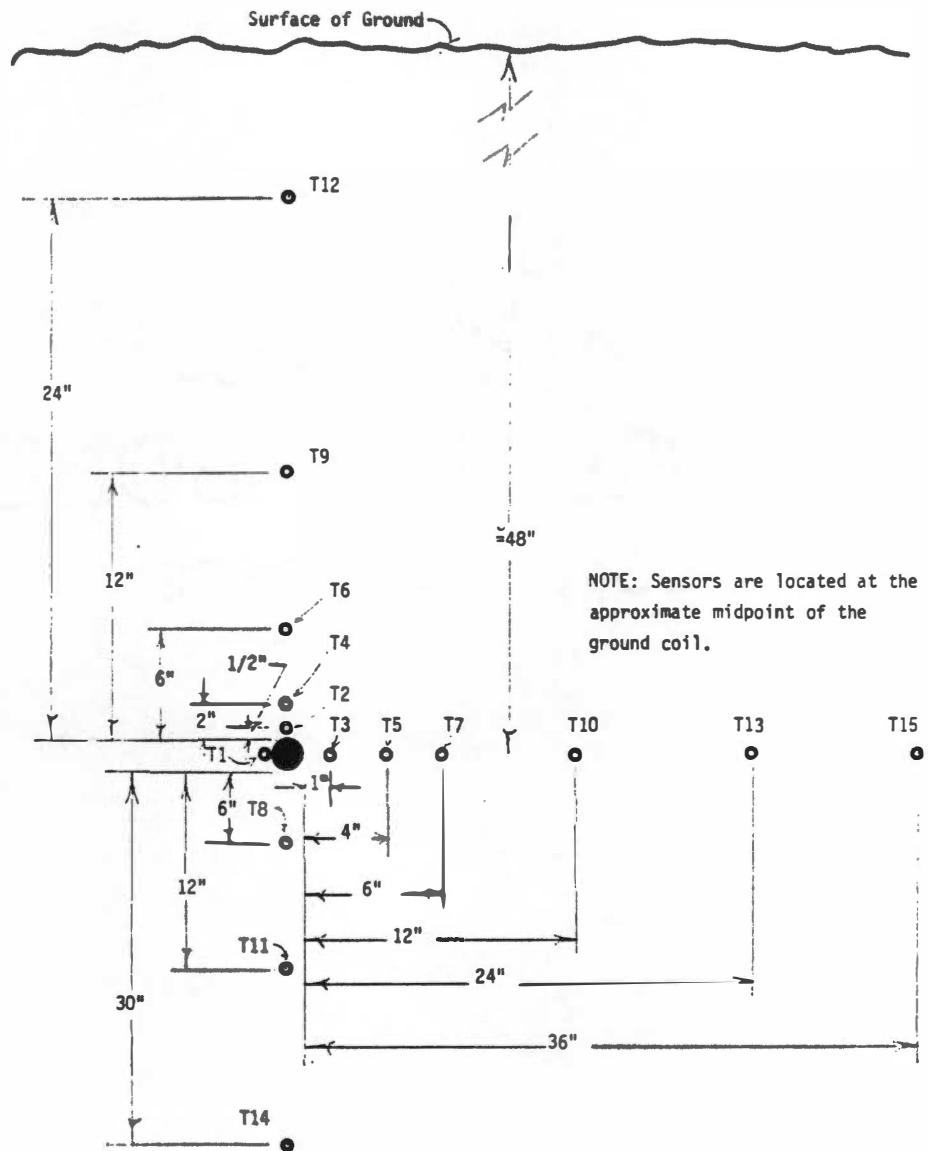
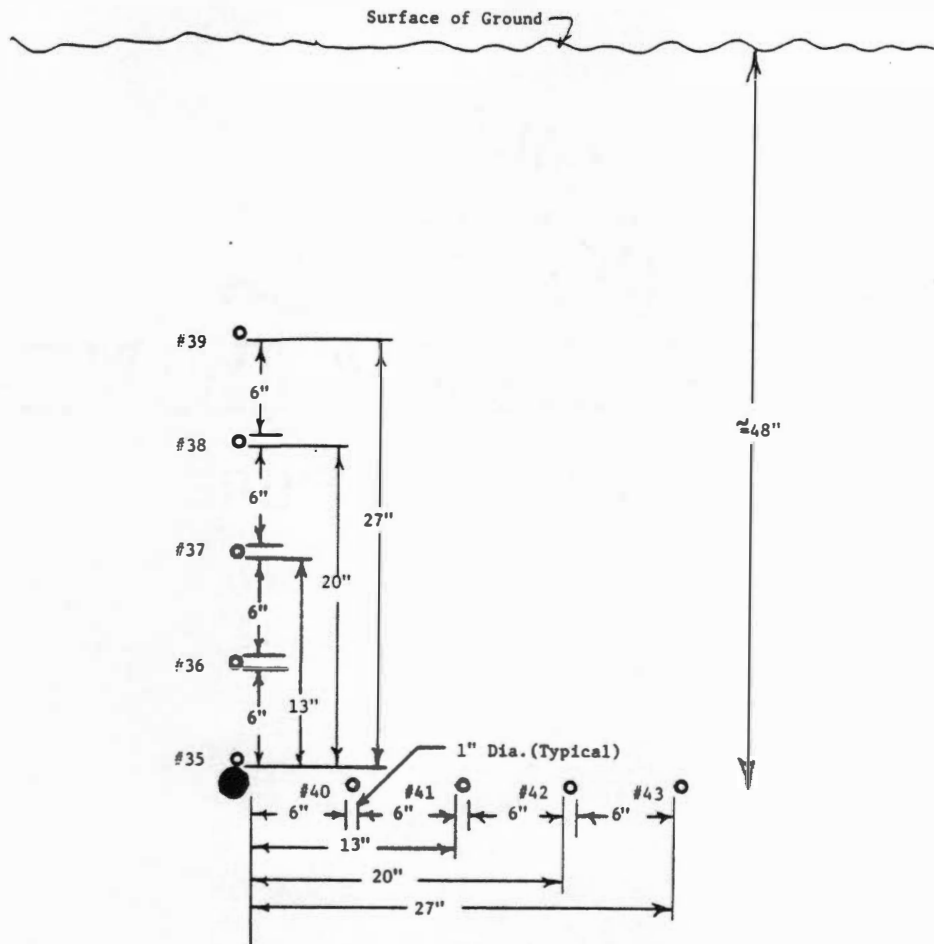


Figure 3-2. Location of Ground Temperature Probes

absolute temperature. The manufacturers data (35) gives an absolute error of 1.0 degrees Celsius over the rated performance range of -55.0 to 150 degrees Celsius.

The temperature measurements of the brine in both circulation loops were made using the temperature sensor used in the energy flow meters. According to Oak Ridge National Laboratory personnel (36), the Winsco PRTD inaccuracies are negligible when compared to other sources of error. The main source of error is the constant current source of the PRTD. The total measurement error in the brine temperatures due to the instrumentation is 0.5 percent.

Soil moisture measurement. Watermark soil moisture sensors manufactured by G.F. Larson Company were used in this research effort. Figure 3-3 presents the location of the moisture sensors relative to the ground coil. The sensors are made of a porous ceramic material which, theoretically, absorbs and releases moisture at the same rate as the surrounding soil. The resistance of the sensor is a function of the moisture within the sensor and can be measured via two electrodes placed within the sensor. Therefore, the



NOTE: Sensors are located at the approximate midpoint of the ground coil

Figure 3-3. Location of Ceramic
Soil Moisture Meters

soil moisture content can be determined by measuring the resistance of the sensor with the assumption that equilibrium is maintained between the sensor and surrounding soil.

An A.C. Wheatstone bridge circuit and a precision adjustable resistance or "decade" box was used to measure the resistance of the soil moisture sensors. This method of measuring sensor resistance gives accurate results if the decade box is an accurate, high quality instrument. The decade box used is accurate to 0.05 percent according to the manufacturer(37).

The calibration data provided by the manufacturer was not based on the percent moisture content of the soil. Therefore, an in-house calibration of the moisture sensors was performed. The calibration procedure consisted of three steps: (1) sample preparation and sensor installation; (2) a measurement of the sensor resistance; (3) determination of the soil moisture content. The soil used in the calibration procedure was taken from the TECH site near the horizontal coil, allowed to dry and crushed to a powder.

Sample preparation consisted of adding a known amount of water to a known amount of soil on a mass basis. The sample was mixed in order to make the sample as homogeneous as possible. The sensor was placed in the soil and the soil was compressed to approximately the soil dry density.

Some problems were encountered with the sample preparation. At low moisture contents, the soil became nonuniform with respect to the moisture distribution. Clumps of soil formed but were broken down as fine as possible during the mixing process.

Compression of the soil sample was also difficult at low moisture contents. A compression on one side of the sample tended to loosen soil on the opposite side of the sample. A wide object was used to compress the sample and solved the soil loosening problem.

The resistance measurement of the sensor was made using the instrumentation discussed previously. A D.C. Wheatstone bridge circuit could cause the moisture sensor to polarize. The polarization of the sensor would cause error in the resistance measurement. An A.C. Wheatstone bridge circuit was used to avoid polarization of the sensor.

Determination of the soil sample moisture content was made using a weight difference technique. A sample of soil near the sensor was taken and weighed. The sample was dried in an oven and the sample weighed again. The difference in weight was taken to be the amount of moisture in the sample. Since the weight of the soil before and after drying and the weight of the water in the sample is known, the moisture content can be calculated.

The calibration curve and calibration points are presented in Appendix C. A least-square line fit was used to generate the calibration curve.

CHAPTER 4

EXPERIMENTAL RESULTS

During the data collection period, a total of 2810 hours of valid data was collected. This corresponds to the heat pump and data collection systems performing adequately for 98 percent of the data collection period of June 6 to October 2, 1983.

The summer of 1983 was approximately average in terms of cooling degree days, but the temperature distribution was skewed. June was a cooler than average month while July and August were warmer than average months. The rainfall was also less than expected for an average summer. A comparison of the weather conditions encountered to the long term average weather conditions is presented in Appendix B.

Heat Pump Performance Data

Table 4-1 presents heat pump performance data for the summer of 1983. Two additional factors, the coefficient of performance (COP) and the seasonal performance factor (SPF) are also presented.

The coefficient of performance is used to determine the thermal performance of a heat pump system. Cooling COP is based on the total or gross amount of cooling

Table 4-1. Heat Pump Performance Data

Week of	Cooling Load (KWh)	Heat Pump Energy Consumption (KWh)	Blower Energy Consumption (KWh)	Pump Energy Consumption (KWh)	COP
6/6/83	98.6	42.1	5.8	4.0	1.90
6/13/83	134.5	54.0	7.8	5.5	2.00
6/20/83	464.6	202.0	32.8	21.5	1.81
6/27/83	453.5	217.6	35.2	22.8	1.64
7/4/83	356.7	173.3	28.2	17.9	1.63
7/11/83	548.1	292.9	45.7	28.8	1.49
7/18/83	588.4	327.7	50.1	31.4	1.44
7/25/83	550.1	312.8	48.9	30.1	1.40
8/1/83	639.8	360.8	53.9	34.3	1.42
8/8/83	541.9	312.1	46.1	29.6	1.40
8/15/83	618.1	354.5	52.7	33.6	1.40
8/22/83	671.2	448.3	65.2	41.6	1.21
8/29/83	473.1	305.1	45.2	29.1	1.25
9/5/83	435.4	261.8	38.6	25.1	1.34
9/12/83	136.2	75.2	10.7	7.0	1.47
9/19/83	72.8	42.3	5.7	3.7	1.41
9/26/83	0.0	10.2	0.0	0.0	0.00

Seasonal Performance Factor: 1.11

provided to the conditioned space. Cooling COP is defined as,

$$\text{COP} = Q_a / W \quad (4-1)$$

where,

Q_a = cooling provided by the heat pump, and
 W = total heat pump system power consumption.

The seasonal performance factor is used to determine heat pump thermal performance on a long term basis. The cooling SPF is based on the net amount of cooling capacity delivered to the conditioned space for the entire cooling season. This means that any internal heat source associated with the heat pump system, such as compressor losses, is subtracted from the total cooling capacity provided to the conditioned space. This can be expressed mathematically as,

$$\text{SPF} = (Q_a - Q_{il}) / W \quad (4-2)$$

where,

Q_{il} = the internal heat sources associated with the heat pump operation.

The experimental SPF for the ground-coupled heat pump system was found to be 1.11 for the 1983 cooling season. The uncertainty in the SPF is +13 percent. The SPF was also estimated with the heat pump system located outside the conditioned space. The compressor and circulation pumps losses were assumed zero in Equation 4-2. This gives an SPF of 1.32, which is an increase of 19 percent in performance by just locating the heat pump system outside the conditioned space.

As can be seen from Table 4-1, there was a system performance deterioration with respect to time. Figure 4-1 illustrates the system performance with respect to time. The uncertainty in the COP is +8 percent. There are three main reasons for the performance deterioration. First, the house cooling load was underestimated during the design phase of the heat pump system. The design cooling load used was 1.41 tons (32) and the actual cooling load is in the range of 2.0 to 2.5 tons(38). The underestimation lead to an undersizing of the ground coil. As long as the actual cooling load is less than the design cooling load, the sizing error is inconsequential. However, when the actual cooling load approaches, then surpasses the design cooling load, system performance deterioration

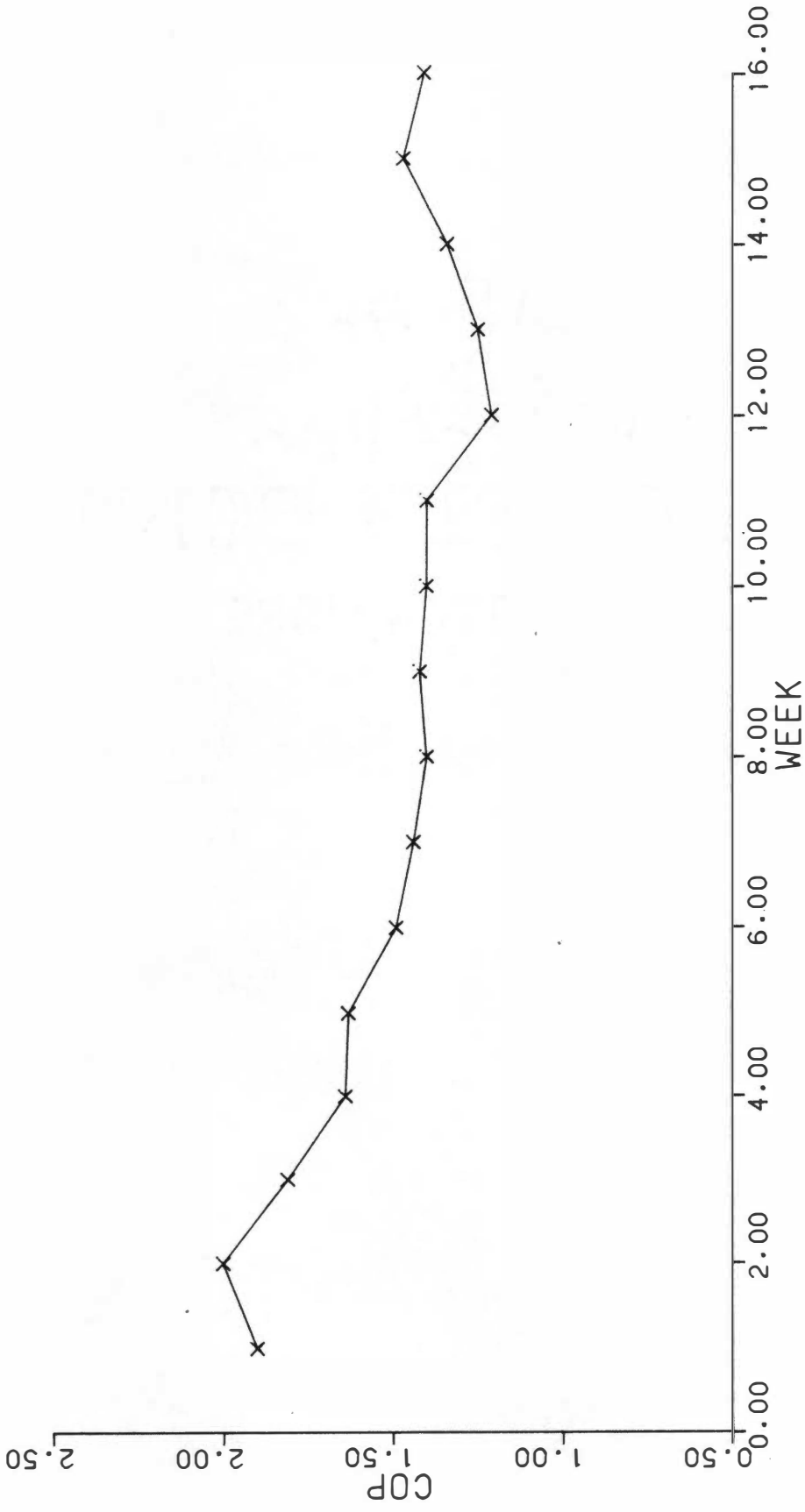


Figure 4-1. Weekly Cooling COPs

occurs. Second, the cooling loads encountered in July and August were larger than expected due to the weather. Third, as the soil dried during the summer, the soil thermal conductivity decreased.

The SPF for the ground-coupled heat pump in this study is poor when compared to the SPF of an air to air heat pump system. For comparative purposes, the SPF for the TECH house III air to air heat pump system was calculated and found to be 2.3. However, the heat pump in TECH house III was not operating under the same conditions as the ground-coupled heat pump. The compressor used in TECH house III is more efficient than the compressor used in TECH house I. The compressor location is also different between the two houses. The compressor used in TECH house III was located outside the conditioned space and the compressor used in TECH house I was located inside the conditioned space. By placing the compressor outside the conditioned space, the internal heat sources are reduced. The reduction of internal heat sources increases the SPF. Therefore, the TECH house III heat pump SPF cited is intended only for a rough comparison of performance.

Experimental Thermal Conductivity

Since the thermal conductivity of the soil can limit the performance of a ground-coupled heat pump, an experimental thermal conductivity of the soil in the region of the ground coil was calculated using experimental temperature and energy flow data. The limitations of the experimental data, such as discrete temperature measurements at one hour intervals, lead to the method used to calculate the experimental thermal conductivity.

The heat transfer from the ground coil to the surrounding soil was modeled as one dimensional radial heat flow through a horizontal cylinder. It was assumed that there was no mass transfer and the material in the control volume was homogeneous. The thermal conductivity within the control volume was assumed to be constant for a given hour of data.

Any transient effects due to heat pump cycling were minimized by using only data that met a certain criterion. The heat pump had to be operating a minimum of 54 minutes during a given hour of data before the data was acceptable. Otherwise, the data was discarded. A total of 769 data points met the criterion.

Since the transient effects were minimized, the heat transfer was considered steady-state. The defining differential equation for the problem previously described is,

$$\frac{d^2 t}{dr^2} + \frac{1}{r} \frac{dt}{dr} = 0 \quad (4-3)$$

The boundary conditions are,

1. $T=T_1$ @ $r=r_i$,
2. $T=T_2$ @ $r=r_o$.

From Krieth (39), the solution for Equation 4-3 and boundary conditions 1 and 2 is,

$$Q_{ss} = 2 * \pi * k * L * (T_i - T_o) / \ln (r_o / r_i) \quad (4-4)$$

where,

Q_{ss} = steady-state heat transfer across the
control volume, (W)

L = length, (m)

k = thermal conductivity, (W/m-C)

r_o = outer radius, (m)

r_i = inner radius, (m)

T_o = temperature at r_o , (C)

T_i = temperature at r_i . (C)

It was necessary to define a control volume in order to use Equation 4-4. The outer boundary of the control volume was taken where the temperature was approximately constant for a given hour of data. Figure 4-2 is a plot of the soil temperature 15.2 centimeters from the ground coil in the horizontal plane. Figure 4-2 reveals that the temperature 15.2 centimeters from the coil is approximately constant for a given hour of data. Therefore, a radius of 15.2 centimeters was taken as the outer boundary of the control volume.

The inner boundary was taken as the inner radius of the coil wall. The average fluid temperature was used for the inner boundary temperature. The average fluid temperature was assumed to be the arithmetic mean of the coil inlet and outlet fluid temperature.

The thermal conductivity of the control volume was calculated for each hour of data that met the runtime criterion. The arithmetic mean of the hourly thermal conductivity data is $0.47 \text{ W/m-C} \pm 8$ percent.

As illustrated from the heat pump power consumption in Table 4-1, the heat pump system did not run the same amount of time each week. Since there was an uneven distribution of the system runtime during the

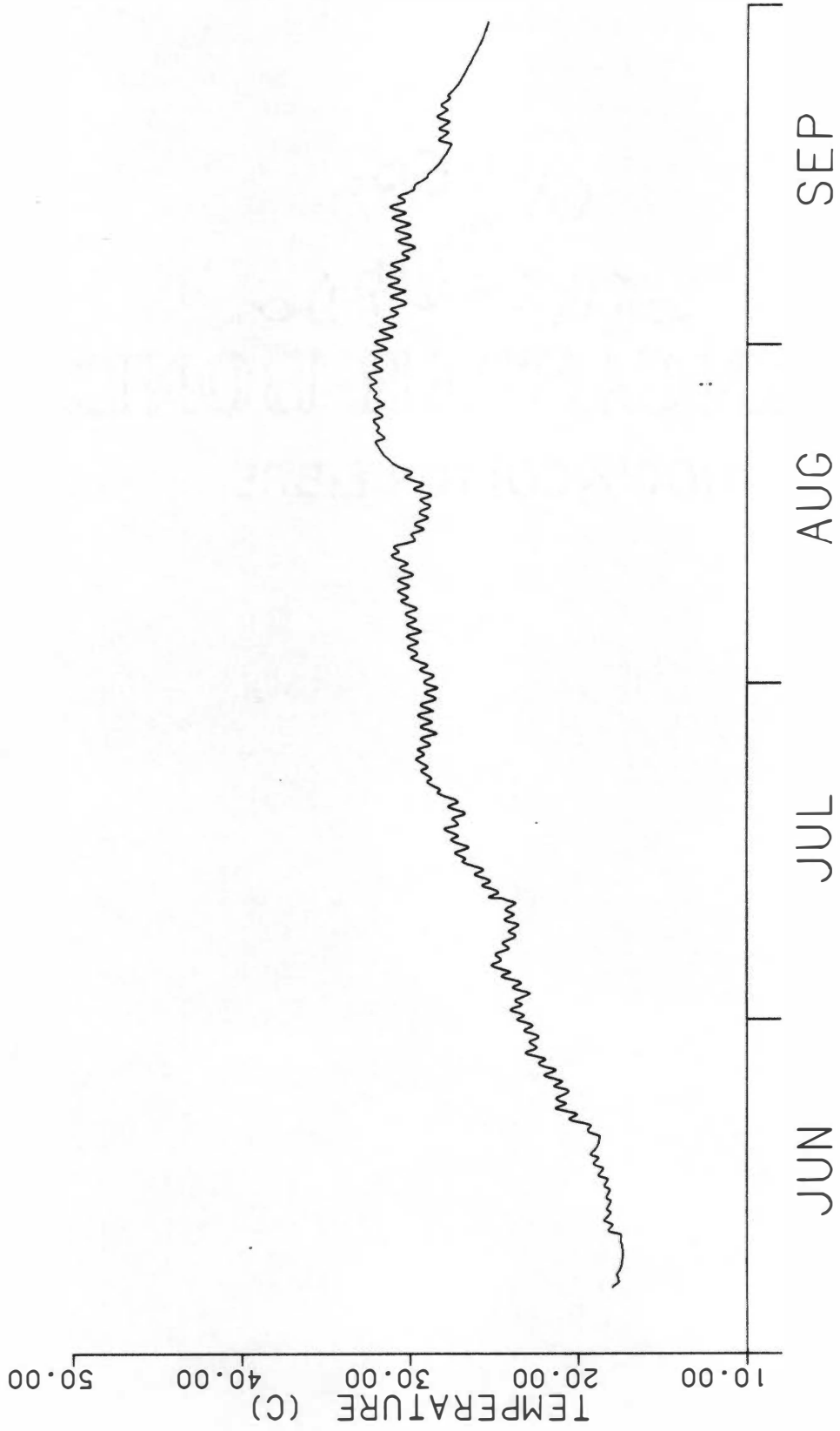


Figure 4-2. Hourly Soil Temperature 15.2 Centimeters from Soil

cooling season, an average seasonal thermal conductivity was calculated from the arithmetic mean of the average weekly thermal conductivities. The average weekly thermal conductivities were calculated by taking the arithmetic mean of the hourly thermal conductivity data for a given week. the average seasonal thermal conductivity based on weekly averages is 0.51 W/m-C +8 percent.

The thermal conductivity of the soil within the control volume was also calculated. Since the control volume is a composite structure, the overall thermal conductivity used in Equation 4-4 is a sum of the individual thermal conductivities. Due to the high coil mass flow rates, the internal film coefficient is considered negligible. Using the electrical analog method described by Krieth (39), the thermal conductivity can be expressed as,

$$\frac{1}{k} \ln\left(\frac{r_o}{r_i}\right) = \frac{1}{k_c} \ln\left(\frac{r_l}{r_i}\right) + \frac{1}{k_s} \ln\left(\frac{r_o}{r_l}\right) \quad (4-5)$$

where,

k_c = coil thermal conductivity,

k_s = soil thermal conductivity,

r_l = coil outer radius.

Equation 4-5 was substituted into Equation 4-4 and the soil thermal conductivity, k_s , was solved for. Only data that met the runtime criterion was used. The average soil thermal conductivity based on hourly thermal conductivities is 0.56 W/m-C ± 8 percent. The average soil thermal conductivity based on average weekly thermal conductivities is 0.63 W/m-C ± 8 percent. Lunardini (25) reports a range of thermal conductivities of 0.12 W/m-C to 1.2 W/m-C. The average soil thermal conductivities calculated previously is within the range of thermal conductivities reported by Lunardini.

In order to check the procedure and assumptions used to calculate the experimental soil thermal conductivity, a comparison with Lunardini's data was performed. At saturation moisture conditions, Lunardini reports a value of 1.2 W/m-C. Lunardini reports an agreement of within 15.0 percent for his fine grain soil thermal conductivities. This gives a range of error of 1.38 W/m-C to 1.02 W/m-C for Lunardini's thermal conductivity data at saturation moisture conditions. From the moisture sensors, saturation moisture conditions were detected for the first week of the cooling season. The experimental

soil thermal conductivity for the first week of the cooling season is $1.05 \text{ W/m-C} \pm 8$ percent. The range of error of the experimental soil thermal conductivity is 1.13 W/m-C to 0.96 W/m-C . Since the ranges overlap, the procedure and assumptions used to calculate the experimental soil thermal conductivity are verified.

Performing a comparison of the average experimental soil thermal conductivity and soil thermal conductivities reported by Lunardini and Sundberg (7) indicate good agreement between the values. Using soil sample data in Appendix D, Lunardini's soil thermal conductivity is 0.95 W/m-C and Sundberg's thermal conductivity is 0.80 W/m-C . Both Lunardini and Sundberg report higher soil thermal conductivities than the experimental soil thermal conductivity, but the difference was expected. As reported in the upcoming soil observations section, void spaces were found adjacent to and in the soil surrounding the ground coil. The void spaces would cause the experimental soil thermal conductivity to be lower than reported soil thermal conductivities.

Figure 4-3 is a plot of weekly experimental soil thermal conductivities. There was no data that met the runtime criterion for the second week. There is a similarity in the trends of the heat pump system

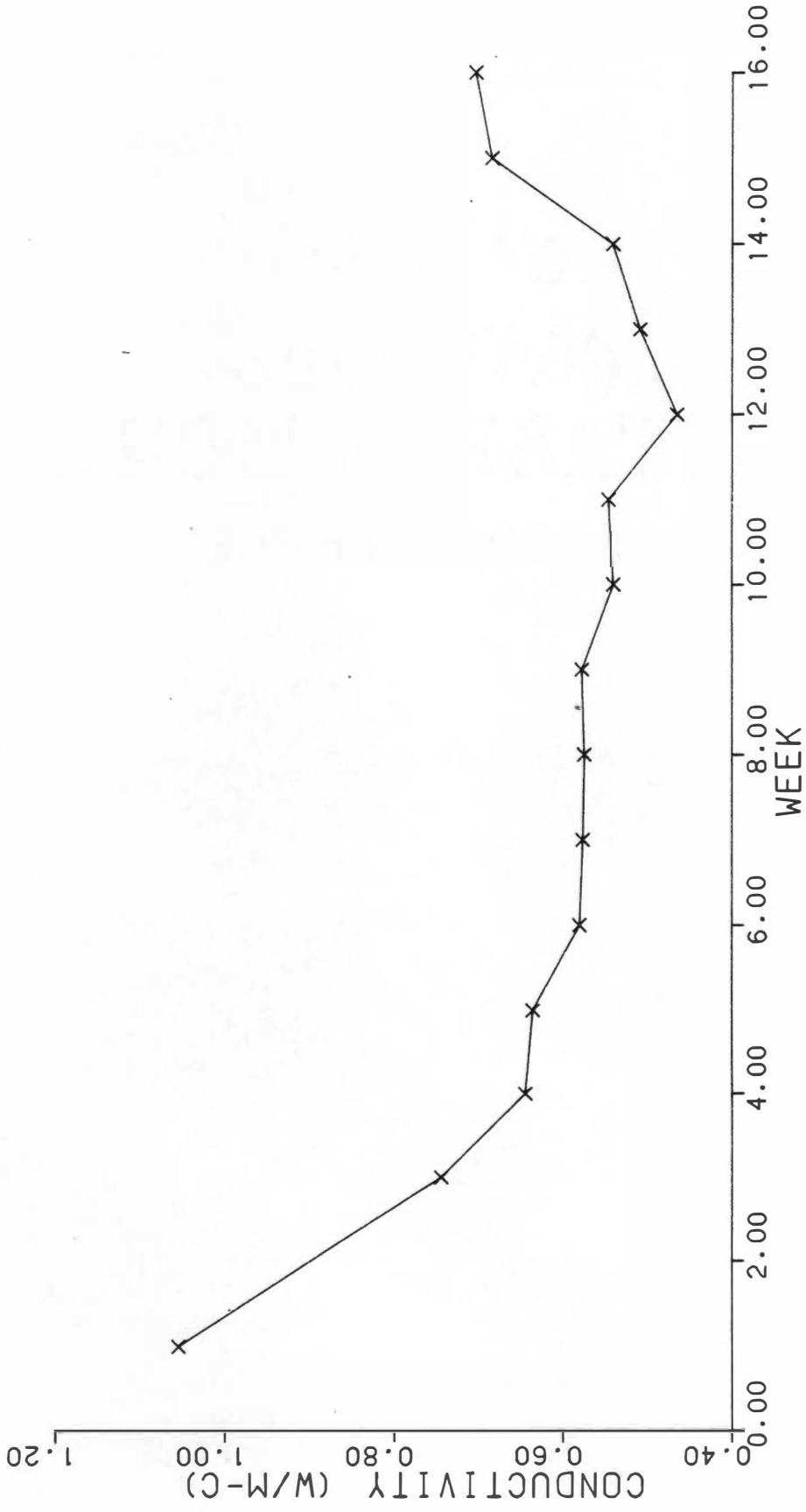


Figure 4-3. Weekly Soil Thermal Conductivity

performance deterioration, Figure 4-1, and the decrease in experimental thermal conductivity, Figure 4-3. Note that when comparing Figures 4-1 and 4-3, the majority of the heat pump performance deterioration occurs at the beginning of the cooling season as does the major portion of change in the thermal conductivity. Also note that between weeks 11 and 12, there is a decrease in the thermal conductivity and a corresponding decrease in heat pump performance. The comparison between the experimental thermal conductivity and the heat pump performance indicates that the soil thermal conductivity is a major contributor toward the heat pump performance deterioration.

Soil Moisture Measurements

Soil moisture measurements were taken at periodic intervals throughout the cooling season. Figure 4-4 presents data from three sensor locations. The sensors used in Figure 4-4 were located adjacent to the coil wall and at a distance 16.5 centimeters from the coil in both horizontal and vertical planes.

As can be seen in Figure 4-4, there was some soil drying throughout the cooling season. Figure 4-4 also shows that the soil next to the coil is drier than at the other locations. This phenomena can be interpreted

as a slight amount of moisture migration from the region directly adjacent to the coil. However, this data was intended only as an indication of the trends of soil moisture, not for absolute values of soil moisture.

Figure 4-5 presents a time average soil moisture profile for July, 1983. In the horizontal plane, there is only a 1.0 percent change in moisture from the 16.5 centimeter location to the 69.9 centimeter location. The majority of the change occurs between the 52.0 centimeter and 69.9 centimeter location in the horizontal plane. The change in moisture with respect to distance from the ground coil is greater in the vertical plane. In the vertical plane, there is a 2.0 percent change in moisture between the 16.5 centimeter location and the 54.6 centimeter location. The approximately constant moisture profile beyond the 16.5 centimeter location suggests that the coil influence on the soil moisture does not extend beyond the 16.5 centimeter location.

The coil influence on the soil moisture in the vertical plane was assumed to not extend beyond the 16.5 centimeter location for three reasons: (1) the influence in the horizontal plane does not seem to

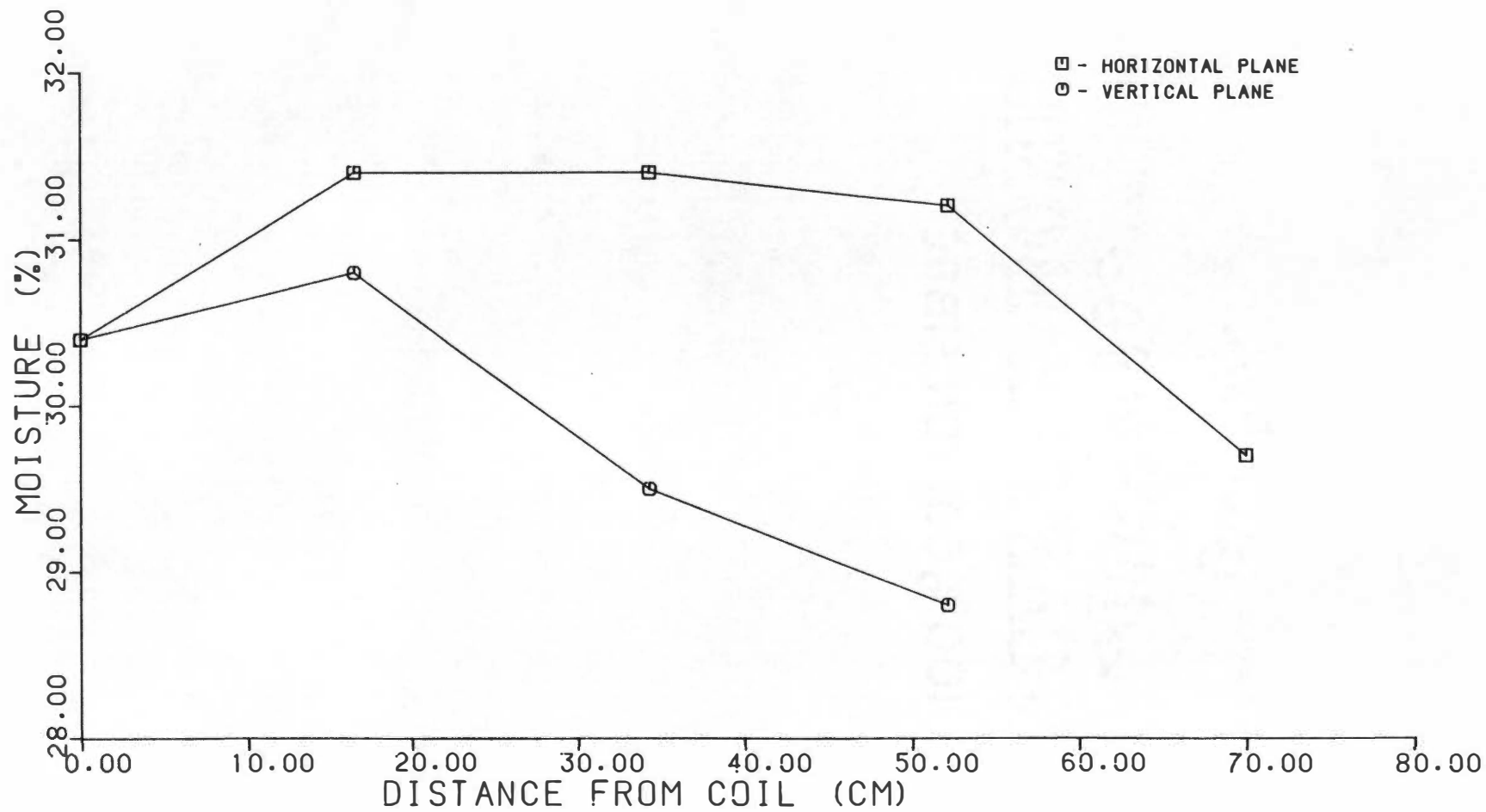


Figure 4-5. July 1983 Time Average Moisture Profile

extend beyond the 16.5 centimeter location; (2) the average moisture content increases from the coil to the 16.5 centimeter location then decreases from the 16.5 centimeter location to the 54.6 centimeter location; (3) the soil in the vertical plane is more susceptible to weather influences than the soil in the horizontal plane.

From the soil moisture observations, the moisture in the region within a 16.5 centimeter radius from the coil is considered to be influenced by both weather effects and coil effects. The moisture in the soil beyond the 16.5 centimeter radius is considered influenced by weather effects only.

Soil Observations

Two soil samples were taken at the TECH site on July 14, 1983. The samples were analyzed for porosity, texture, percent moisture, density, and several other soil properties. One sample was taken in the trench where the coil was buried and the second sample was taken in nearby undisturbed soil. The soil was found to be approximately 85 percent clay and silt and 15 percent sand. A detailed description of the soil is presented in Appendix D.

A hole was dug in the coil field on August 9, 1983, in order to inspect the ground coil and surrounding soil. As the hole was dug, air gaps were observed at the interface between the soil in which the coil was buried, designated disturbed soil, and the surrounding undisturbed soil. The gaps at the interface occurred intermittently from the surface to the coil. Several other air spaces were encountered in the disturbed soil as the hole was dug.

After the hole was dug, an air gap approximately 5.1 centimeters long and 0.63 centimeters wide was discovered parallel to and in contact with the coil wall. This air gap occurred where the coil approached the interface between the disturbed and undisturbed soil and was not evident when the coil was in the middle of the disturbed soil.

The soil in contact with the top of the coil was light in color and dry to the touch in several locations. In other locations along the top of the coil, the soil was darker. Along the bottom of the coil the soil was dark in color and plastic to the touch. Soil color is an indication of moisture content since, for a given soil, the darker the soil, the greater the moisture content.

On October 2, 1983, a second hole was dug in a different location from the hole dug in August. The interface was not as distinct as the interface of the hole dug in August. Air gaps were not encountered as the hole was dug. The soil was well packed and moist to the touch in the vicinity of the coil.

Soil Thermal Stability

The phenomena of soil thermal stability discussed in Chapter 2 must be addressed in designing ground-coupled heat pumps for cooling. If the soil adjacent to the coil is thermally unstable, then a rapid drying will occur. The soil thermal conductivity will approach the dry soil thermal conductivity as the soil dries resulting in the degradation of the performance of the heat pump. Soil thermal stability is dependent on the level of the heat flux and the initial moisture content of the soil. Obviously, a thermally stable soil is desirable adjacent to the coil.

The data from Black, Hartly, et al., (40) was used in an attempt to determine if the soil adjacent to the ground coil was thermally stable or unstable. Data for a sample of Georgia red clay at 20.0 percent moisture

content was used. The lowest heat flux used by Black, Hartly, et al., was 51 W/m and the time to reach the point of thermal instability is greater than 84.7 hours.

The observed daily average energy flow to the ground was approximately 25 W/m for the ground coupled heat pump. Since there was no data at 25 W/m, the question of thermal stability cannot be answered at this time. From experimental data gathered by the moisture sensors, the soil does not appear to reach the point of rapid drying. The effects of a cyclic heat flux on soil thermal stability has not been explored so it cannot be said that the soil adjacent to the ground coil is thermally unstable.

CHAPTER 5

MODEL COMPONENTS AND RESULTS

As mentioned previously, the TRNSYS and GROCS computer programs were used to model the ground coupled heat pump system. TRNSYS version 10.1 was used to model the heat pump system and GROCS was used to model the ground thermal performance.

Model Description

TRNSYS is a FORTRAN language compiler designed to connect component models of transient systems and solve the resulting algebraic and differential equations that describe the system. Each component model of the system is formulated as a separate FORTRAN subroutine. Some of the component models presently available with TRNSYS include flat plate solar collectors, room models and heat exchangers. The components used from TRNSYS to model the ground-coupled heat pump system are a data reader, a pump, a fan, a heat pump, an interface with GROCS and printers.

The components are connected by a series of inputs and outputs that are similar to the pipes, wires, etc., that connect the physical system components. Operating

parameters of the components, such as heat pump performance curves, and user-supplied data, such as weather data, are combined with the component configuration to produce a transient system. TRNSYS then simulates the system performance by calling the component subroutines until all the system algebraic and differential equations converge. To solve simultaneous algebraic and time dependent differential equations, TRNSYS uses a Modified Euler integration algorithm. The algorithm is a first order predictor-corrector algorithm that uses Euler's method for the predicting step and the trapezoid rule for the corrector step. One advantage in using the Modified Euler integration algorithm is that the iterative calculations occurring during a single timestep are performed at a constant time value. This allows the algebraic equations to converge by successive substitution as the iteration required to solve the time-dependent differential equations progresses(41).

Heat pump. The heat pump subroutine supplied with TRNSYS offers several different modes of operation for maximum flexibility. The heat pump is capable of using either air or water heat sinks and sources. The

flexibility of the subroutine allows the heat pump to be tailored to the users needs.

To use the heat pump model, the user must supply performance data over a range of operating temperatures. The performance data are the energy rejected by the condensor, energy added to the evaporator and compressor work. The performance data are found during a simulation run by linear interpolation. Since the heat pump used in this research effort was a heating-only heat pump, cooling performance data were not readily available from the manufacturer. Experimental data were used as the heat pump performance data in the model.

The heat pump subroutine performs at quasi-steady state conditions, that is, the heat pump performs at steady state conditions for a given timestep. In order to use experimental performance data, a criterion was used to minimize transient effects. The heat pump had to operate for a minimum of 60 percent of a given hour before the data was considered. If a higher percent of runtime was used as the criterion, performance data at low temperatures could not be established. The performance curves used in this research effort are presented in Appendix E.

The heat pump model must meet three conditions for operation in the cooling mode: (1) The model has an input for a signal from a controller, in effect, an on/off switch. The switch must be in the "on" position; (2) The cooling load must be greater than zero; (3) Mass flow through the heat pump must be greater than zero.

For simulation runs in this study, the on/off switch in condition one was in the "on" position at all timesteps. A constant input value placed the switch in the "on" position. The second and third conditions were met from inputs to the program.

GROCS. GROCS is a FORTRAN computer program developed at Brookhaven National Laboratory (8) and was designed to simulate three dimensional underground heat flow. Initial validation of GROCS was reported by Metz (9,10) who compared experimental data and model predictions. GROCS was used in this study because the program was available, had some evidence of validation and was compatible with TRNSYS.

GROCS was designed to solve a set of finite difference equations over a series of "blocks" of earth. Each block is a volume of soil whose size,

shape, location and interaction with other blocks are determined by the user. The details of each block are determined from a hand drawn model of the ground coupling device to be simulated. Figure 5-1 presents the block arrangement used in this study.

Two types of blocks are used in GROCS, "rigged" blocks and "free" blocks. The temperature of each free block, once initialized, is determined at each timestep by the thermal interaction of the block in question and the surrounding blocks. A subroutine within GROCS determines the temperature of the rigged blocks at each timestep from a user supplied table of monthly average soil temperatures as a function of depth. A method presented by Kusuda (42) for calculating soil temperatures as a function of depth was used in this study. Since the rigged blocks surround the free blocks, realistic temperature boundary conditions are provided at all timesteps in the simulation.

Two modifications were performed to GROCS in order to enhance the capabilities of the program. GROCS originally allowed only 20 free blocks for any simulation. The number of free blocks was increased to 50. GROCS would also allow only one thermal conductivity for the entire field under consideration.

The program was modified to allow each block, free and rigged, to have an individual thermal conductivity.

Input and output data. Two data inputs were used in the model runs in this study. The inputs were the experimental cooling load per hour and the system percent runtime per hour. Both inputs were read from a data file via the TRNSYS data reader once per hour of simulation time. The cooling load was fed into the appropriate input of the heat pump model, thus satisfying the second condition for heat pump operation. The system percent runtime was used to turn on the circulation pump. With the circulation pump operating, the third condition for heat pump operation was satisfied. The heat pump operated until the cooling load was met.

The outputs from the model were the energy to the ground, the power consumption of the heat pump, circulation pumps and fan, the coil inlet and outlet temperatures and the amount of energy transferred to each block adjacent to the ground coil. Each output was printed on an hourly basis for the simulation run.

Model Verification

Three model outputs were compared with experimental data to verify the accuracy of the computer model. These factors are the coil inlet and outlet temperatures, the energy rejected to the ground and the heat pump power consumption. Figures 5-2 and 5-3 are the coil inlet and outlet temperature comparisons respectively. The differences between the model and experimental data are thought to come from two sources. One, the model used a constant soil thermal conductivity for the entire cooling season while the experimental thermal conductivity varied. A variable soil thermal conductivity was not used so maximum flexibility of the model would be maintained. If a variable thermal conductivity was used, the way in which the soil thermal conductivity varied would have to either be known or assumed by the user before a simulation and would have to be some type of input to the model. Simulations of a ground-coupled heat pump in other regions would be very difficult since this information is not readily attainable from conventional sources of weather data such as the National Weather Service.

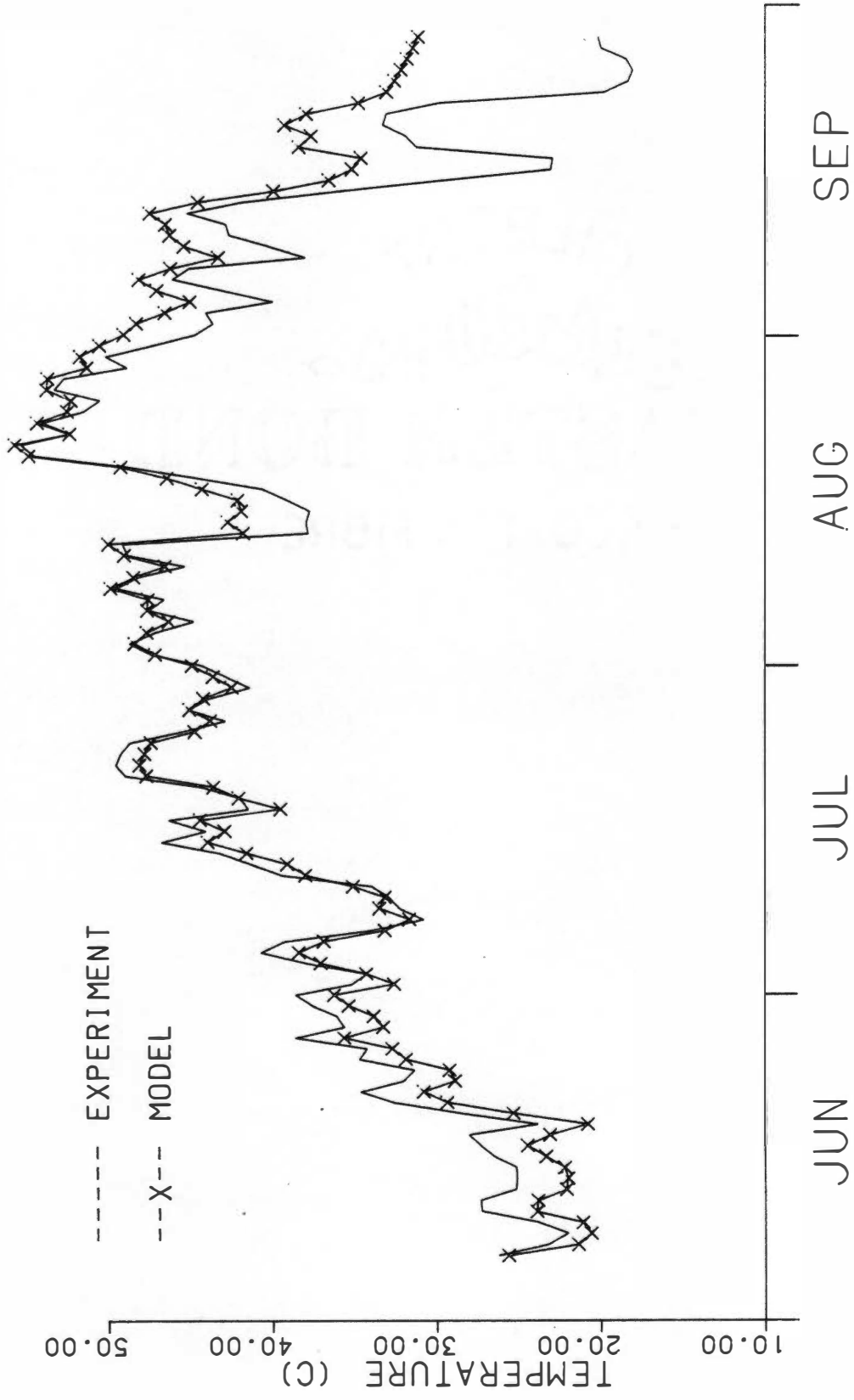


Figure 5-2. Coil Inlet Temperature Comparison

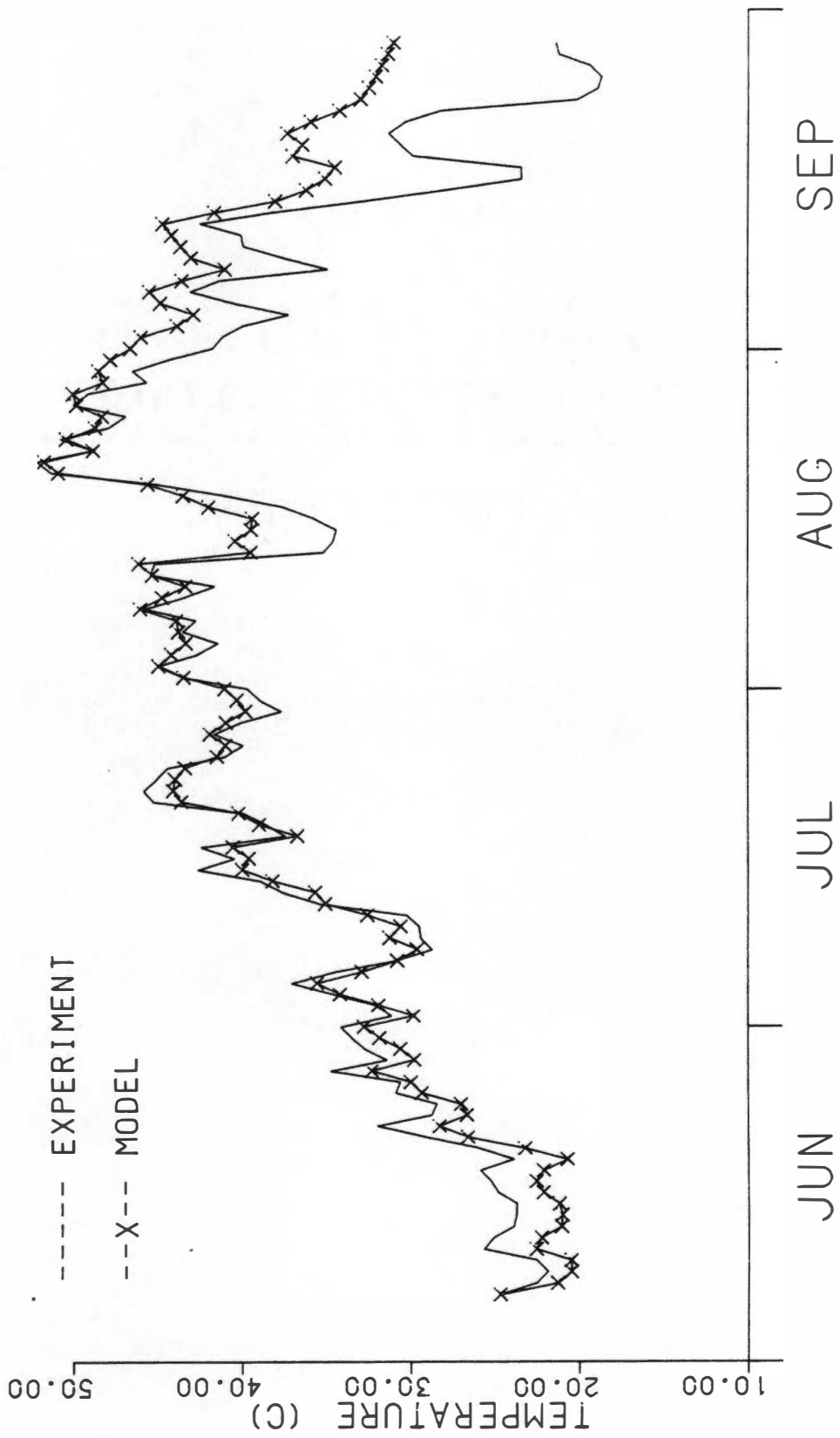


Figure 5-3. Coil Outlet Temperature Comparison

The second source of error between the model and experimental temperatures has to do with the positioning of the temperature sensors. The model takes the coil outlet temperature to be the average of the calculated ground temperatures adjacent to the ground coil. The temperature sensors inside the ground coil were located in the conditioned space so when the heat pump was off the temperature seen by the sensors would start approaching the conditioned space temperature. This affect is most noticable in September when the heat pump was operating infrequently.

Figures 5-4 and 5-5 are comparisons between the experimental data and the model predictions. Figure 5-4 compares the energy rejected to the ground and Figure 5-5 compares the heat pump power consumption. There is an excellent agreement between the experimental data and the model predictions. The agreement between the experimental data and the model predictions validate the use of the model in predicting heat pump performance under various conditions.

Three values of soil thermal conductivity were used in the validation of the model. The blocks of soil adjacent to the coil were within the control

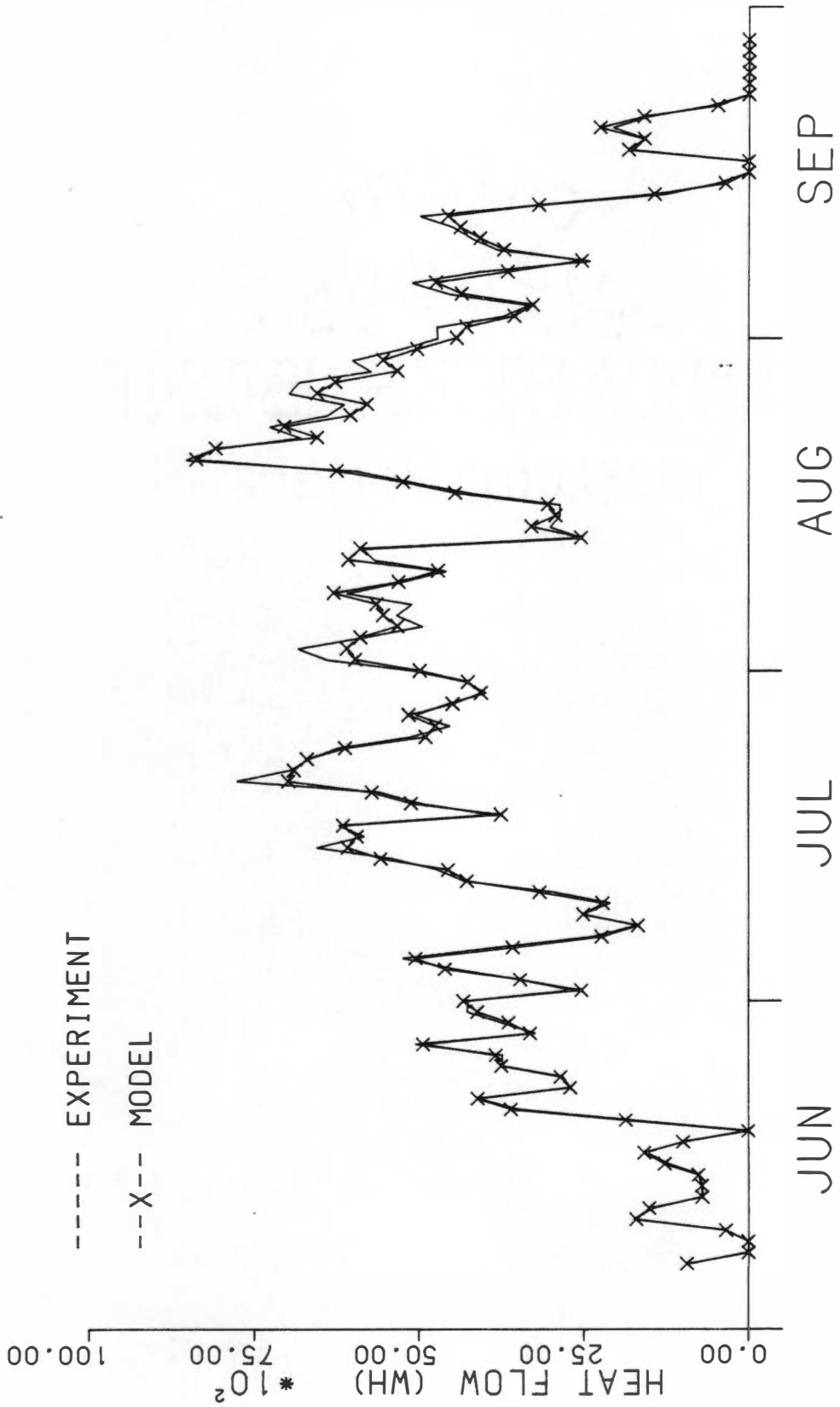


Figure 5-4. Energy to Ground Comparison

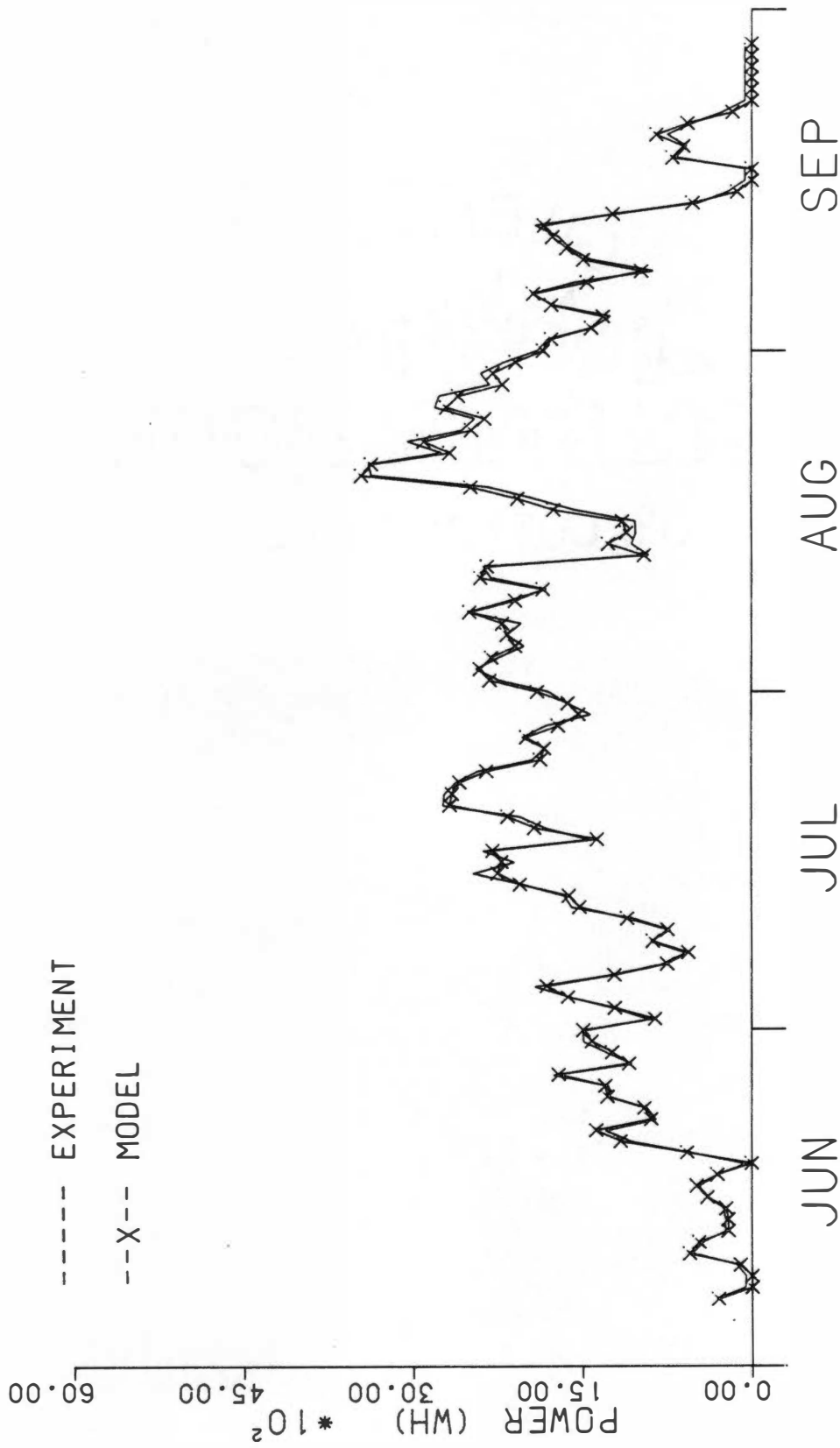


Figure 5-5. Heat Pump Power Comparison

volume defined in calculating the experimental thermal conductivity. The most logical choice for the thermal conductivity in this region was the experimental thermal conductivity.

The blocks of soil outside the control volume were assigned a thermal conductivity from Lunardini's data(25). The selection of the value was based on the soil core sample data presented in Appendix D.

Several blocks of soil were partially inside the experimental soil thermal conductivity control volume. These blocks were given a weighted average value between the experimental thermal conductivity and the thermal conductivity of the blocks outside the control volume.

Parametric Studies

From the excellent comparison between the experimental data and the model prediction, it was decided to determine the SPF of a ground-coupled heat pump under varying soil parameters. The effects of soil density and moisture content of both fine grained and course grained soils on the SPF were addressed. Also, the effect on the SPF by varying the cooling load was calculated. The maximum performance for a

ground-coupled heat pump in the Knoxville area was also estimated.

Moisture effects. The moisture content of both fine and course grained soil were varied from saturation to a low moisture content, 2 percent for course grained soil and 5 percent for fine grained soil. The corresponding thermal conductivity at each moisture content was used in the model and was taken from Lunardini's data(25).

Figure 5-6 presents the effect on the SPF of varying the moisture content. Note that the largest change in SPF occurs at low moisture contents. This behavior was expected since the thermal conductivity change with moisture is greater at lower moisture contents than at higher moisture contents. Note also that, for a given moisture content, the SPF using the course grained soil thermal conductivity is always higher than the SPF using the fine grained soil thermal conductivity. This phenomena is due to the higher value of thermal conductivity of the solid material of the course grained soil when compared to the thermal conductivity of the solid material of the fine grained soil. Quartz is the main component of sand and has a

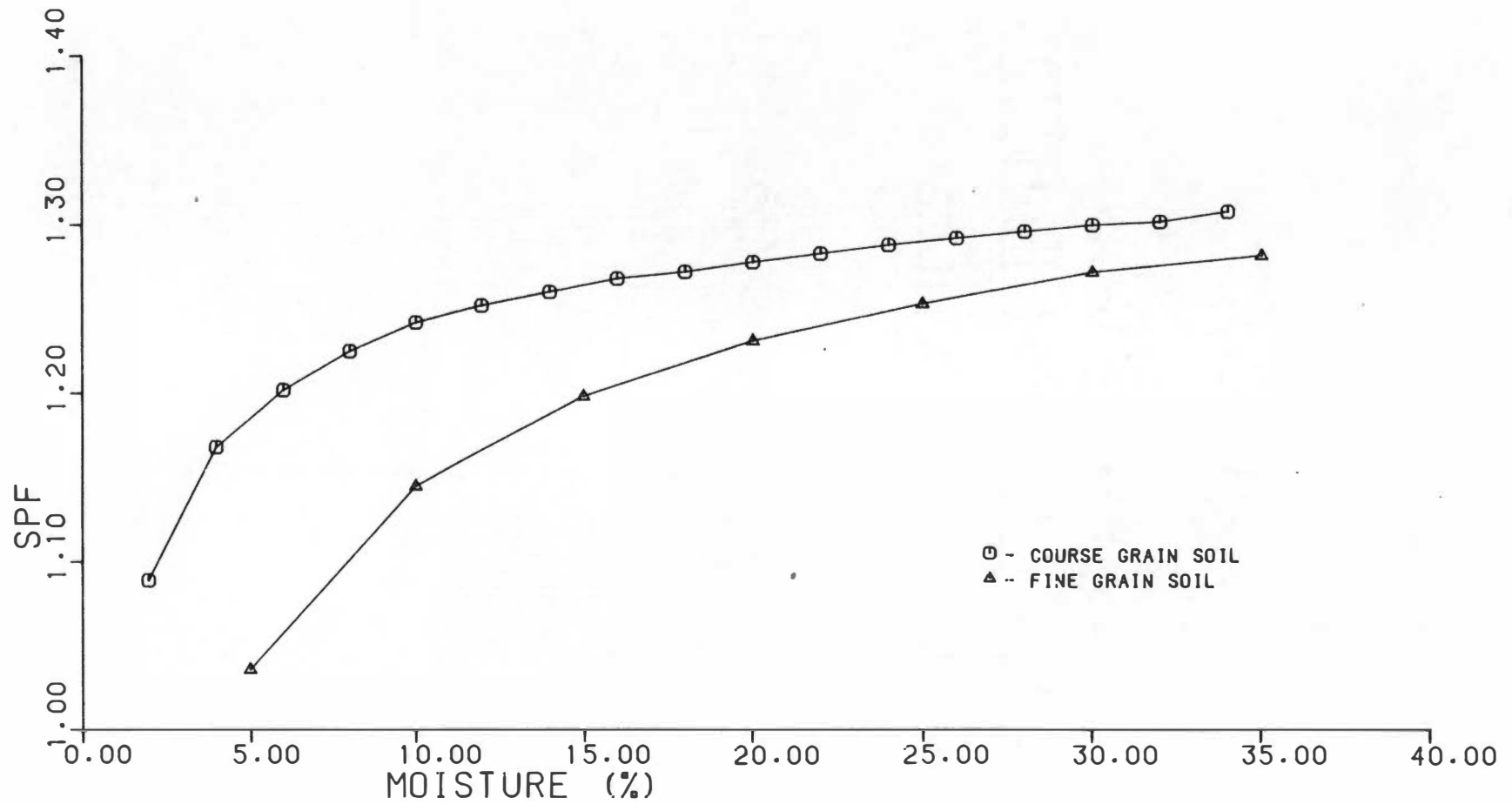


Figure 5-6. Moisture Effects on SPF

higher thermal conductivity than the solid material in fine grained soils. The model predicts there would be a maximum increase in the SPF of 16 percent over the experimental SPF. This would occur if the soil were coarse grained and at saturation conditions.

Density effects. The density of both coarse and fine grained soil were varied over a wide range. Corresponding values of thermal conductivity were also taken from Lunardini's data(25). Figure 5-7 presents the effect of density changes on the SPF. As with the moisture content effects, the coarse grained soil gives a higher SPF than the fine grained soil for a given density. This is due to the previously explained difference in the solid material thermal conductivity. The model predicts an approximately linear increase in the SPF as the density increases for both types of soil. The model also predicts a maximum increase of 18 percent in the SPF over the experimental SPF.

Cooling load effects. The effect of reducing the cooling load or increasing the coil length on the SPF was also predicted using the model. An experimental cooling load per unit coil length was found to be 33.0 KWh/m. The cooling load per unit coil length was determined by dividing the total seasonal cooling

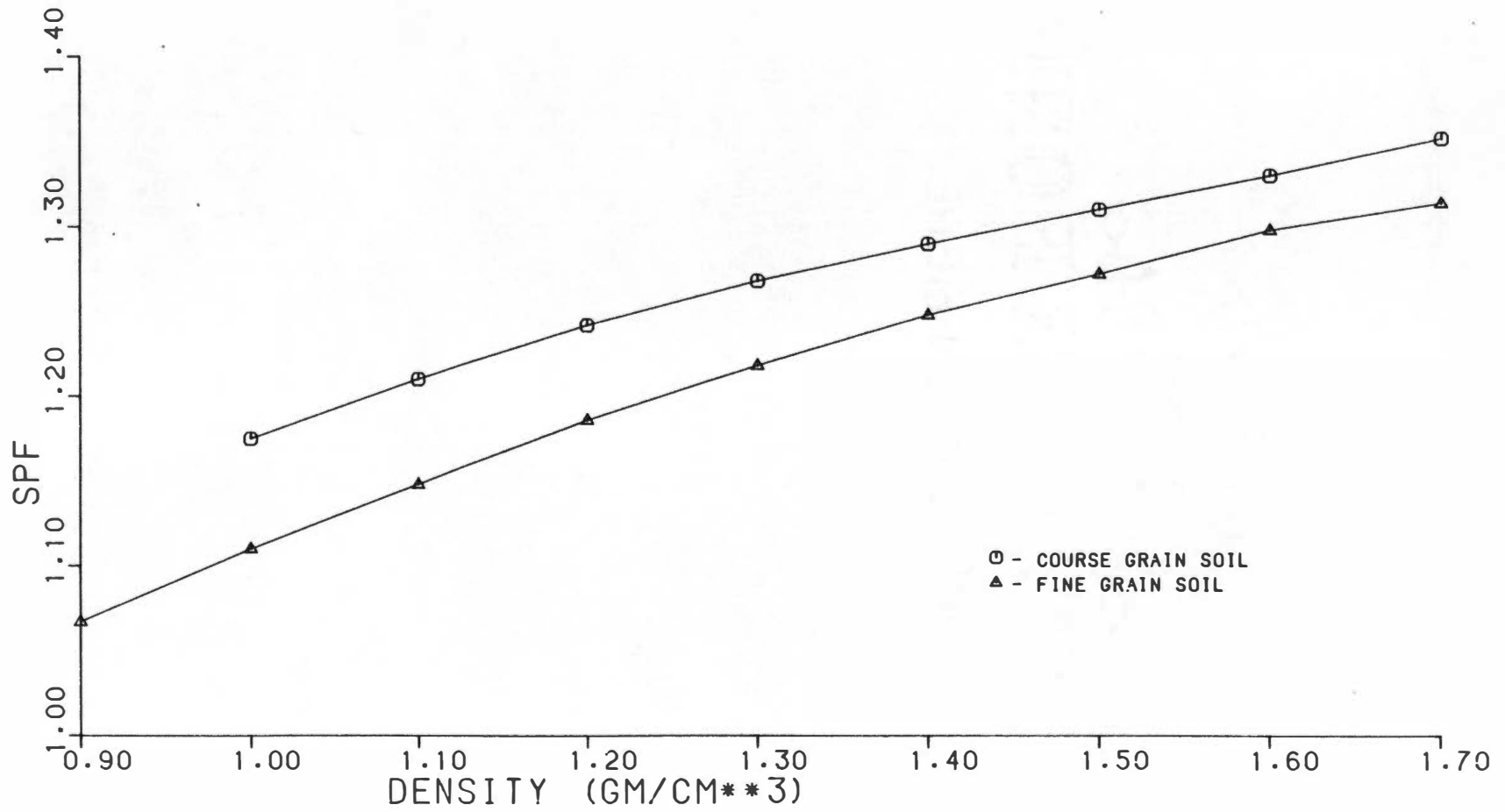


Figure 5-7. Density Effects on SPF

provided by the heat pump by the total coil length. The cooling load per unit coil length was varied between 3.3 KWh/m and 66.0 KWh/m. Figure 5-8 presents the predicted SPF verses the cooling load per unit coil length.

The high moisture soils performed much better than the low moisture soils over a wide range of cooling loads per unit coil length. In the region of low cooling loads per unit coil length (<8.25 KWh/m), the soil thermal properties start losing significance in the heat transfer process. This was expected since, as the coil length approaches an infinite length, the coil outlet temperature approaches the far-field soil temperature regardless of the coil inlet temperature. This trend is illustrated in Figure 5-9. Therefore, the far-field soil temperature is a limit on the performance of the ground-coupled heat pump.

Figure 5-8 gives an idea of the best possible SPF for the heat pump system and weather conditions used in this study. The maximum SPF predicted by the TRNSYS-GROCS model was between 1.4 and 1.6.

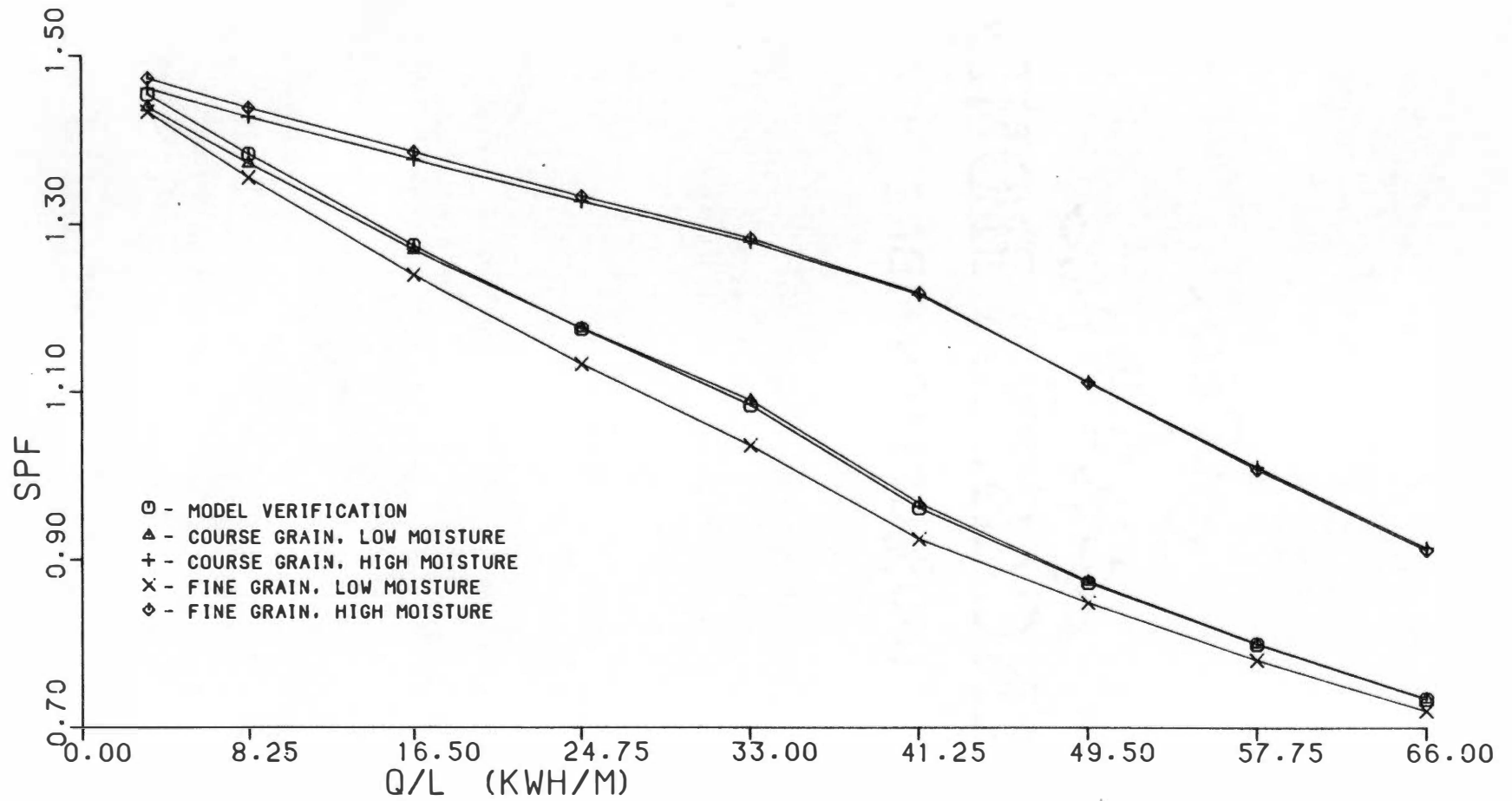


Figure 5-8. Cooling Load Effect on SPF

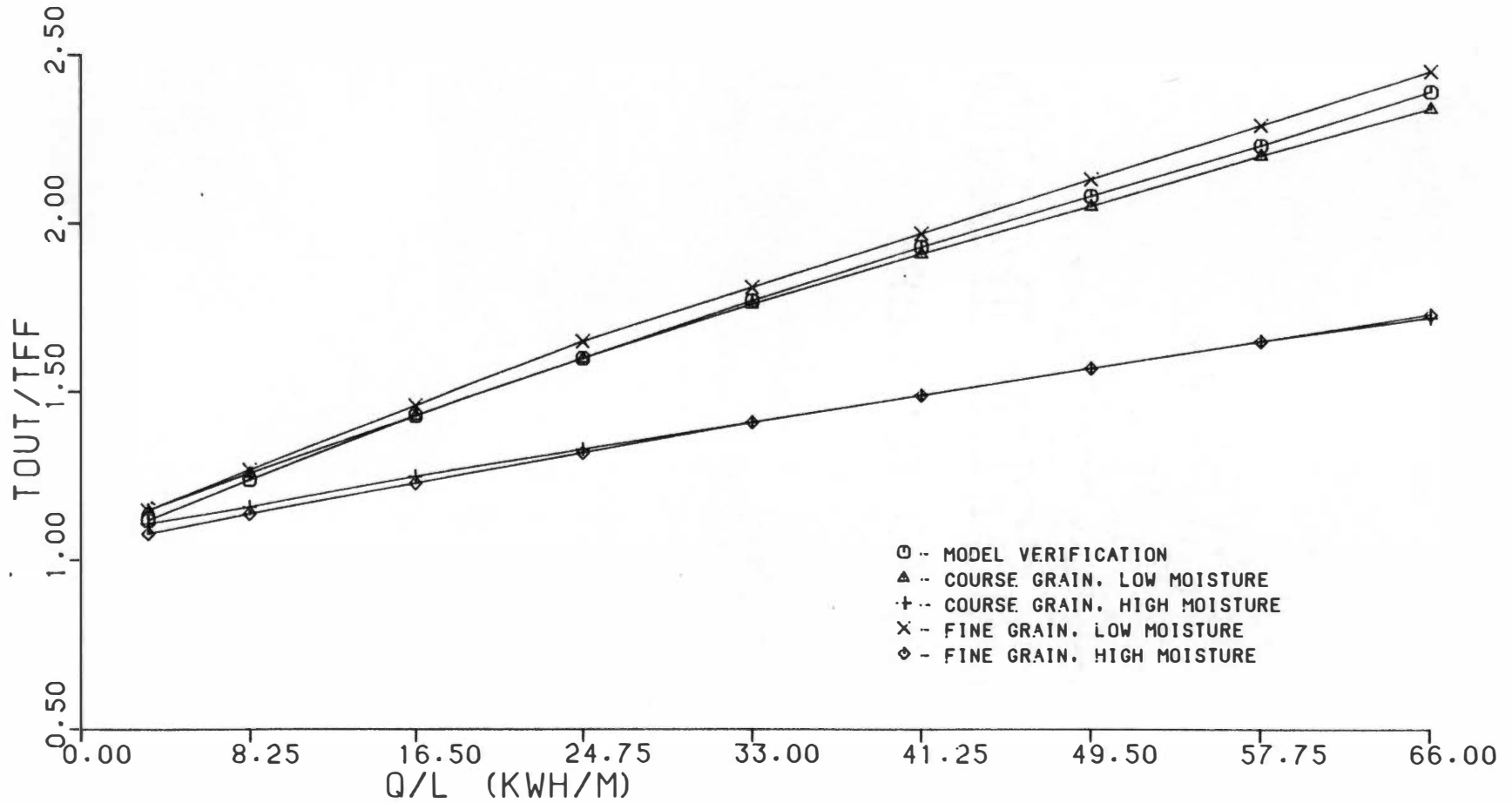


Figure 5-9. Coil Outlet Temperature vs Cooling Load

Far-field effects. The model was also run using far-field data for two other locations. The locations chosen were Tyler, Texas and Argonne, Illinois. For the Texas location, the average summer far-field temperature at a 1.22 meter depth was increased from 20.9 C to 25.6 C. The 23 percent increase in temperature caused a 6 percent decrease in the SPF. For the Illinois location, the far-field temperature was decreased from 20.9 C to 16.0 C. The 23 percent decrease in the far-field temperature resulted in a 5 percent increase in the SPF.

Maximum predicted performance. The TRNSYS-GROCS model was used to predict the maximum performance of a ground-coupled heat pump system in the Knoxville area. Performance data for an Entercon II water source heat pump was used(43). The Entercon II heat pump COP was 3.46 at 30 C which is a 32.6 percent increase in performance over the TETCO heat pump. The TETCO heat pump COP was 2.61 at 30 C. Since performance data for the Entercon heat pump was given only at one temperature, it was assumed that the performance curves of both heat pumps were parallel. In order to compensate for the design error mentioned in Chapter 4,

the cooling load per unit coil length was reduced by 30 percent. Bose rule of thumb (5) of 106 meters per ton of cooling was used since design procedures for a ground-coupled heat pump are sparse. The soil used was a well packed, coarse grained soil at saturation moisture conditions. These soil conditions give the maximum value for soil thermal conductivity. Soil thermal conductivity was taken from Lunardini's data (25) for the previously mentioned soil conditions. The resulting SPF predicted by the model was 1.87. This represents an increase of 68 percent over the experimental SPF of 1.11.

The heat pump performance was also predicted with the system outside the conditioned space. An SPF of 2.04 was predicted using the aforementioned conditions. This represents an increase of 84 percent over the experimental SPF.

CHAPTER 6

CONCLUSIONS AND RECOMENDATIONS

This study has shown that the ground-coupled heat pump used in this study performed inadequately during the cooling season. The experimentally determined SPF of 1.11 is poor by any standard. Four factors detract from the performance. The first factor is the placement of the heat pump system in the conditioned space. Placing the system outside the conditioned space should result in an SPF of 1.32 due to the reduced internal loads. In the heating season, however, placement of the heat pump inside the conditioned space is desirable since system losses reduce the house heating load. For the optimum location of the heat pump system, performance during both seasons must be examined.

The second factor is the soil thermal conductivity adjacent to the ground coil. Comparing the experimental thermal conductivity with the system COP reveal similar trends with respect to time. A decrease in thermal conductivity produced a decrease in COP. Three recommendations to increase the soil thermal conductivity are: (1) Backfill the trench with a

course grain soil; (2) Install a watering system to keep the soil at saturation conditions; (3) Pack the soil in the trench to increase density and reduce void spaces.

The third factor is soil thermal stability. Instrumentation did not detect the rapid drying that is characteristic of a thermally unstable soil. Since the instrumentation was located at only one point along the coil, it is possible that the soil in other locations was thermally unstable. Observations of the soil on the upper half of the coil showed patchy areas of dry soil. Moisture detection instrumentation along the length of the coil and data collection every hour is recommended. Tensiometers similar to those in use by Oak Ridge National Laboratories (44) are a possibility. Experimental work into soil thermal stability and the effects of a cyclic heat flux is recommended.

The fourth factor is the ground coil used in this study was undersized for cooling. The ground coil was sized for a cooling load of 1.41 tons (32) while the actual cooling load was in the range of 2.0 to 2.5 tons(38). Taking the worst case cooling load, 2.5 tons, and Bose recommendation (5), the coil should be increased by at least 61 meters.

An additional instrumentation recommendation is for several more temperature sensors installed along the coil length and a distance less than 16 centimeters from the coil. The additional temperature data would provide information on the soil temperature gradient and the temperature change along the length of the coil.

This study has also shown that the TRNSYS-GROCS computer model is an excellent representation of the ground-coupled heat pump during the cooling season. A development of a model of TECH house I is recommended. The house model would allow predictions of ground-coupled heat pump performance throughout the world.

Parametric studies using the model predicts that the best performance of a ground-coupled heat pump occurs in densely packed, saturated coarse grained soil. The worst performance predicted occurs in loosely packed, dry, fine grained soil.

How the SPF changed as soil moisture content or density changed was predicted. Four conclusions were made from the results: (1) As moisture or density increased, the SPF increased. As moisture content or density decreased, the SPF decreased; (2) The rate of

change of SPF due to moisture content change was dependent on the moisture content. The majority of SPF change occurred at moisture contents between zero and 15 percent; (3) The rate of change of SPF due to density change is approximately linear; (4) For a given density and moisture content, coarse grain soil performs better than fine grain soil.

SPF changes due to varying the seasonal cooling load per unit coil length were predicted. Three conclusions from the results are made: (1) A decrease in the seasonal cooling load per unit length produces an increase in the SPF. An increase in the seasonal cooling load per unit length produces a decrease in the SPF; (2) High moisture soil performs better than low moisture soil regardless of the grain size; (3) The SPF for all soil types and moisture contents approaches a single value between 1.4 and 1.6 as the cooling load per unit length approaches zero.

The model was used to predict far-field temperature effects on the SPF. The ground-coupled heat pump is not highly sensitive to changes in the far-field temperatures. A change of 23 percent only changed the SPF by 5 to 6 percent.

The model was also used to predict the maximum performance of a ground-coupled heat pump in the Knoxville area. The model predicted an SPF of 1.87 with the heat pump within the conditioned space. With the heat pump system outside the conditioned space, the model predicts a maximum SPF of 2.04. With the SPF in the range of 1.87 to 2.04, the ground-coupled heat pump has the potential of being competitive with air type heat pumps.

LIST OF REFERENCES

LIST OF REFERENCES

1. McGuigan, D., Heat Pumps-An Efficient Heating and Cooling Alternative, Garden Way Book Co., 7-8, 1981
2. American Society of Heating, Refrigeration and Air Conditioning Engineers, Systems and Equipment Guide and Data Book, 607-611, 1967
3. Briggs, J.B. and Shaffer, C.J., "Seasonal Heat Pump Performance for a Typical Northern United States Environment", E.G. and G. Idaho, Inc., 1979
4. Kemler, E.N. and Oglesby, C.H., Heat Pump Applications, McGraw-Hill Book Company, 127-131, 1950
5. Bose, J.E., "Water Source HVAC System Design Briefing", School of Technology and Technology Extension, Oklahoma State University, 1981
6. Edison Electric Research Bulletin, "Research Results Concerning Earth as a Heat Source or Sink", 355-357, 1953
7. Nordic Symposium on Earth Heat Pump Systems, Goteborg, Sweden, 1979
8. Metz, P.E., "A Simple Computer Program to Model 3-Dimensional Underground Heat Flow with Realistic Boundary Conditions", ASME Transactions, Vol 105, 42-49, 1983
9. Metz, P.E., "The Use of Ground Coupled Tanks in Solar Assisted Heat Pump Systems", Proceedings, ASME 4th Annual Solar Energy Division Conference, 128-136, 1982
10. Metz, P.E., "The Use of Serpentine Earth Coils in Ground Coupled Heat Pump Systems", Proceedings, ASME 5th Annual Solar Energy Division Conference, 452-461, 1983
11. Klein, S.A., Beckman, W.A. and Duffie, J.A., "TRNSYS- A Transient System Simulation Program", Solar Energy Laboratory, University of Wisconsin, Madison, Report 38, 1979

12. Brady, N.C., The Nature and Properties of Soil, Macmillan Publishing Company, 12-16, 1974

13. Schwab, G.O., Frevert, R.K., Edminster, T.W. and Barnes, K.K., Soil and Water Conservation Engineering, John Wiley and Sons, Inc., 118-128, 1966

14. Soil Survey Staff, "Soil Classification- A Comprehensive System- 7th Approximation", U.S. Department of Agriculture, 1960

15. Soil Survey Staff, "Supplement to Soil Classification System- 7th Approximation", U.S. Department of Agriculture, 1967

16. DeVries, D.A., Physics of Plant Environment, North Holland Publishing Co., 210-235, 1963

17. Bracht, J., "Über die Wärmeleitfähigkeit des Erdbodens und des Schnees und den Wärmeumsatz im Erdboden", Veroff, Geophys. Inst. Univ, Leipzig, 2, Ser, 14 Heft 3, 1949

18. Lang, C., "Über die Wärmekapazität der Bodenkonstituenten, Forschung Gebiete", Agrikultur-Physik 1, 109, 1898

19. Ulrich, R., "Untersuchungen Über die Wärmekapazität der Bodenkonstituenten", Forschung Gebiete, Agrikultur-Physik 17, 1, 1894

20. DeVries, D.A., and DeWitt, D.E., "Die thermischen Eigenschaften der Moorboden und die Beeinflussung der Nachtfrostgefahr dieser Bodendurch eine Sanddecke", Met. Rundschau 7, 41-45, 1954

21. Kersten, M.S., "Thermal Properties of Soil", University of Minnesota, Institute of Technology Engineering Experiment Station Bulletin, No 28, 1949

22. Walker, W.R., Sabey, J.G., and Hampton, L.M., "Studies of Heat Transfer and Water Migration in Soils", Colorado State University, Department of Agriculture and Chemical Engineering, Fort Collins, Co, 1981

23. Gemant, W.O., "The Thermal Conductivity of Soil", Journal of Applied Physics, Vol 21, 750-752, 1950

24. Hartly, J.G. and Black, W.Z., "Transient Simultaneous Heat and Mass Transfer in Moist, Unsaturated Soils", Journal of Heat Transfer, Vol 103, 376-382, 1981

25. Lunardini, V.J., Heat Transfer in Cold Climates, Van Nostrand Reinhold Company, 147-174, 1981

26. Phillip, J.R. and DeVries, D.A., "Moisture Movement in Porous Material Under Temperature Gradients", Transactions, American Geophysical Union, Vol 38, No 2, 222-232, 1957

27. Rose, C.W., "Water Transport in Soil with a Daily Temperature Wave", Australian Journal of Soil Research, Vol 6, 45-47, 1968

28. Sepaskhah, A.R. and Boersma, L., "Thermal Conductivity of Soils as a Function of Temperature and Water Content", Soil Science Society of America Journal, Vol 43, 439-444, 1979

29. Hadas, A., "Evaluation of Theoretically Predicted Thermal Conductivities under Field and Laboratory Conditions", Soil Science Society of America Journal, Vol 41, 460-466, 1977

30. Cary, J.W., "Water Flux in Moist Soil: Thermal vs Suction Gradients", Soil Science, Vol 100, No 3, 168-175, 1965

31. Johnson, W.S., McGraw, B.A., Bedinger, A.F.G., Conlin, F. and Wix, S.D., "Interim Report 2- November 1, 1982- April 30, 1983", Oak Ridge National Laboratory, Contract No. Carbide Sub 7685 PA X92, 1983

32. Fischer, R.D. and Newman, D.C., "Design of the Ground-Coupled Heat Pump System for the UT Soar House", Battelle Report to Oak Ridge National Laboratory, Conservation Technology, 1981

33. Blevins, D.P., Knoxville Utility Board, Knoxville, Tennessee, Personal Communication, 1983

34. Briggs, B., Minco Corporation, Mineapolis, Minnesota, Personal Communication, 1983
35. Analog Devices Catalog, 6-8, 1983
36. Miller, D., Oak Ridge National Laboratory, Oak Ridge, Tennessee, Personal Communication, 1983
37. Electro-Measurements, Inc., Portland, Oregon, Instrument Label, 1983
38. McGraw, B.A., Energy, Environmental and Resources Center, University of Tennessee, Knoxville, Tennessee, Personal Communication, 1983
39. Krieth, F., Principles of Heat Transfer, Intext Educational Publishers, New York, 3rd Ed., 1973
40. Black, W.Z., Hartly, J.G., Martin, M.A. and Bush, R.A., "Practical Aspects of Applying Soil Thermal Stability Measurements to the Rating of Underground Power Cables", IEEE Transactions on Power Apparatus and Systems, Vol PAS-100, 1981
41. TRNSYS Users Manual, Version 10.1, Solar Energy Laboratory, University of Wisconsin, Madison, Wisconsin, 1979
42. Kusuda, A. and Achenback, P.R., "Earth Temperatures and Thermal Diffusivity at Selected Stations in the United States", ASHRAE Transactions, Vol 71 Part 1, 61-74, 1965
43. Air Conditioning and Refrigeration Institute, "Directory of Certified Applied Air Conditioning Products", Vol 54, Dec 1, 1983- May 3, 1984
44. Shimshi, D. and Michel, J.W., "The Effect of Various Rates of Semicontinuous Drip Irrigation on Lettuce (*Lactuca sativa* L.) Grown in a Greenhouse", Oak Ridge National Laboratory, 1973
45. Kline, S.J. and McClintock, F.A., "Describing Uncertainties in Single-Sample Experiments", Mechanical Engineering, 75, No 1, 3-8, 1953

46. Knoxville Weather Service, Personal
Communication, 1983

47. Girard, J.P., Geotek Engineering Company, Soil
Sample Results, 1983

APPENDICIES

APPENDIX A

EXPERIMENTAL ERROR ANALYSIS

Energy Flow Uncertainty

The energy flows were experimentally determined by the following expression,

$$Q = k * F_{\text{flow}} * F_{\text{delt}} \quad (1)$$

where,

Q=measured energy flow,

k=calibration constant,

F_{flow}=flowmeter signal frequency,

F_{delt}=temperature signal frequency.

The uncertainty in the energy flows can be determined using an uncertainty analysis proposed by Kline and McLintock(45). The uncertainty in the energy flow can be expressed as,

$$\frac{U_q}{Q} = \left[\left(\frac{U_k}{K} \right)^2 + \left(\frac{U_{\text{flow}}}{F_{\text{flow}}} \right)^2 + \left(\frac{U_{\text{delt}}}{F_{\text{delt}}} \right)^2 \right]^{1/2} \quad (2)$$

where,

$U_q, U_k, U_{flow}, U_{delt}$ = uncertainties of the energy flows, calibration constant, flowmeter signal frequency, and temperature signal frequency, respectively.

For the brine to air coil and the ground coil energy flow measurements, the following uncertainties were used,

$$U_k/k = 7.4\%$$

$$U_{flow}/F_{flow} = 0.5\%$$

$$U_{delt}/F_{delt} = 1.0\%$$

Using Equation 2, an uncertainty of ± 7.4 percent was calculated for both energy flows.

Electric Power Uncertainty

According to KUB personnel(33), the maximum error expected in the electric power meters is ± 0.5 percent. The maximum error associated with the data acquisition system is ± 0.5 percent. This will give a total error of ± 1.0 percent for the electric power measurements.

Temperature Sensor Uncertainty

The maximum error associated with the inlet and outlet temperatures of the brine to air coil and the ground coil is ± 0.5 percent(36). The error is due to the accuracy of the constant current source used in reading the temperature sensors. The error of the temperature sensors is negligible(36). Therefore, the error of the temperature measurements in the brine to air coil and the ground coil is ± 0.5 percent.

According to the manufacturer, the maximum error associated with the ground temperature sensors is ± 0.7 percent(34). Including the error associated with the data acquisition system, the total error of the ground temperature measurements is ± 1.2 percent.

APPENDIX B

WEATHER DATA

1. Summer 1983 Weather Conditions

Month	June	July	August	September
Degree Days	235	425	462	217
Temperature (C)	22.5	25.8	26.4	21.3
Rainfall (mm)	73.4	53.6	42.9	16.3

2. Long Term Mean Weather Conditions

Month	June	July	August	September
Degree Days	283	391	372	209
Temperature (C)	23.5	25.3	25.0	21.9
Rainfall (mm)	100.3	110.0	76.7	75.9

Source: Reference 46

APPENDIX C

MOISTURE METER CALIBRATION CURVE

The calibration data provided by the manufacturer was not based on percent moisture content of the soil. It was decided to perform an in-house calibration which resulted in the following calibration curve. Three moisture meter sensors were used in the calibration. Details of the calibration procedure are in Chapter 3.

The calibration curve is only for Watermark ceramic soil moisture meters manufactured by G.F. Larson company.

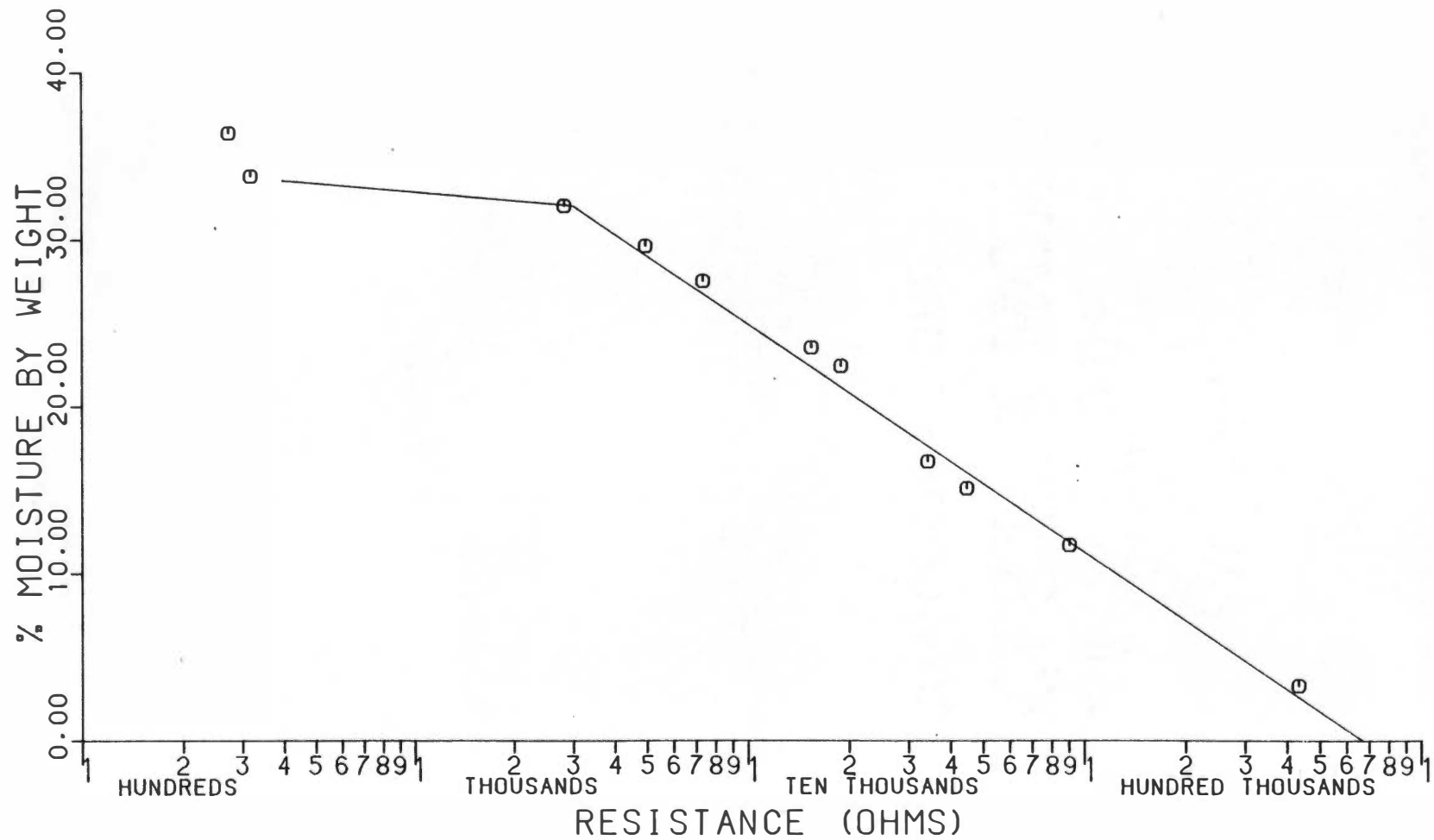


Figure C-1. Moisture Meter Calibration Curve

APPENDIX D

SOIL SAMPLE DATA

	Disturbed Soil	Undisturbed Soil
Porosity:	52.8%	35.0%
Wet Density:	1571.4 Kg/m	1997.5 Kg/m
Natural Moisture:	24%	17%
Degree of Saturation:	54.4%	78.0%
Liquid limit:	42%	34%
Placticity Index:	16	13
<u>Soil Texture</u>		
Clay and Silt:	85%	87%
Sand:	15%	13%
Source:	Reference 47	
Volumetric Heat Capacity:	2109.7 Kj/m ³ C	2394.4 Kj/m ³ C

Note: Volumetric heat capacity calculated using
Equation 2-5

APPENDIX E

HEAT PUMP PERFORMANCE CURVES

Experimental data was used to generate the following heat pump performance curves. The experimental data used were the energy taken from the conditioned space, the energy added to the ground and the energy consumption of the compressor.

In order to use the experimental data, a criterion was used to minimize transient effects. The heat pump had to operate a minimum of 60 percent of an hour before the data was considered usable. If a higher percent runtime was used, performance data at low temperatures could not be established.

The data that met the runtime criterion was grouped in one degree Celcius increments. The arithmetic mean of the data within the increment was used as the performance data. For example, the data between 34.5 C and 35.5 C was averaged and used as the performance data at 35.0 C. A least squares technique was used to generate the curves.

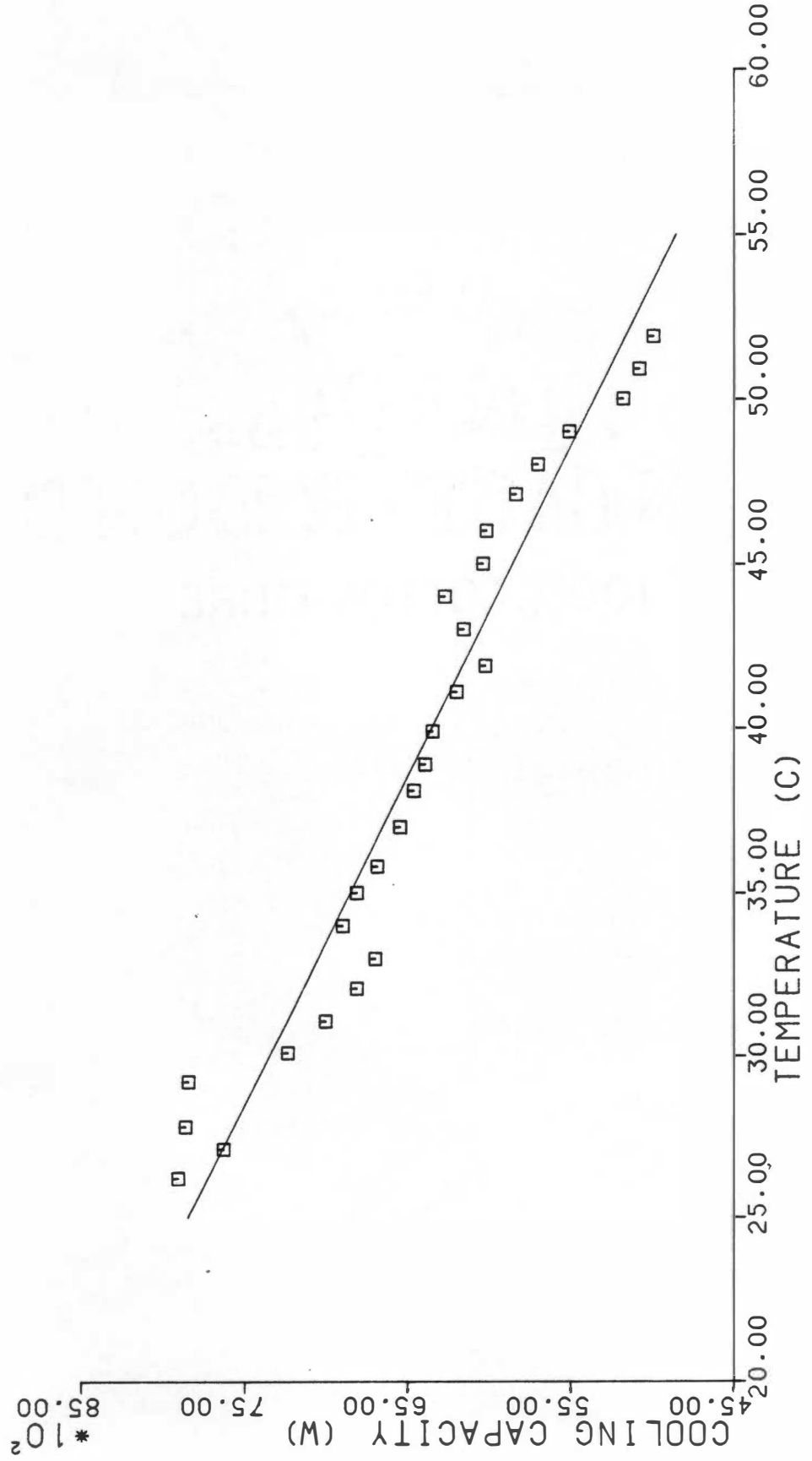


Figure E-1. Temperature vs Cooling Capacity

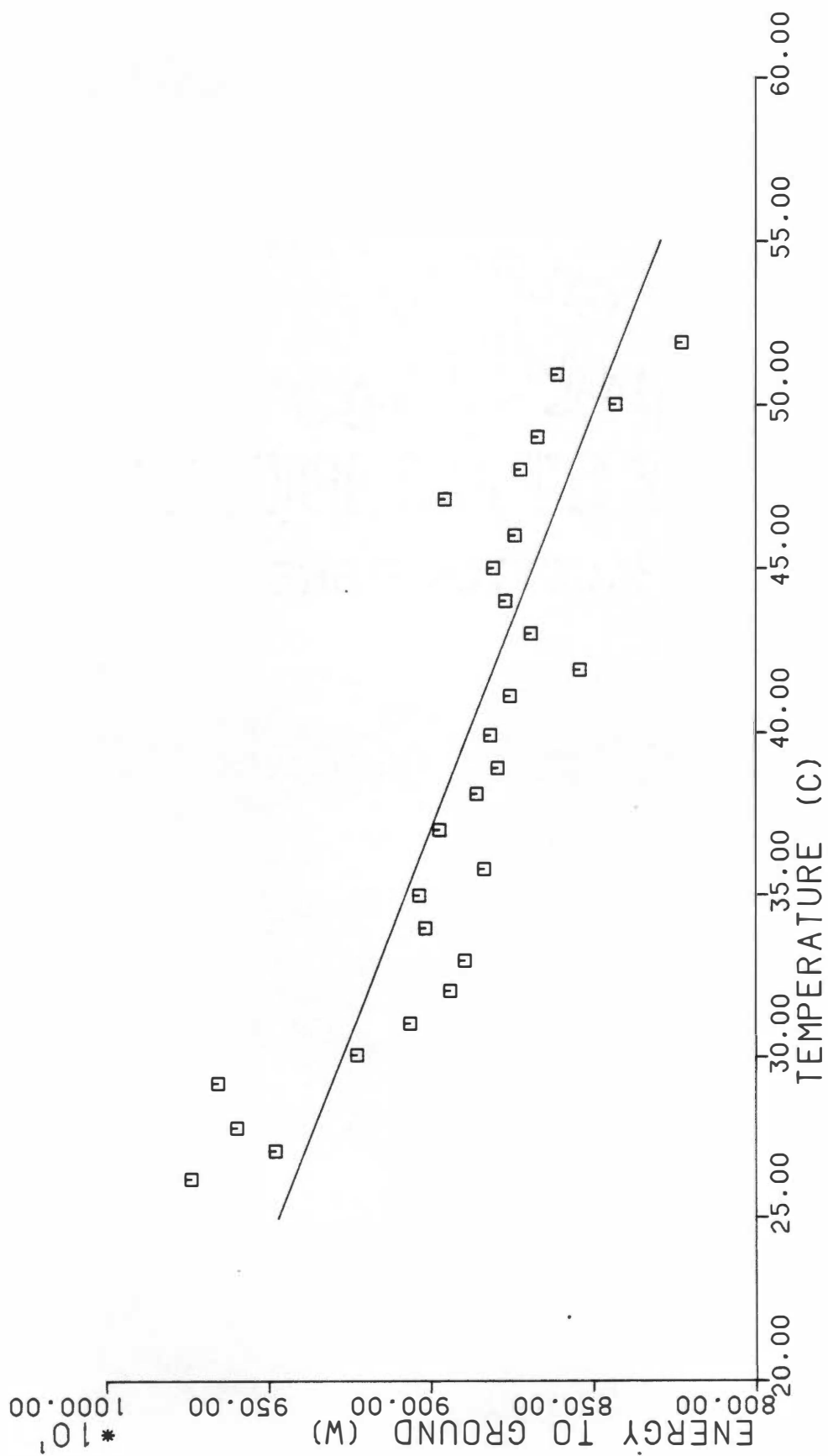


Figure E-2. Temperature vs Energy to Ground

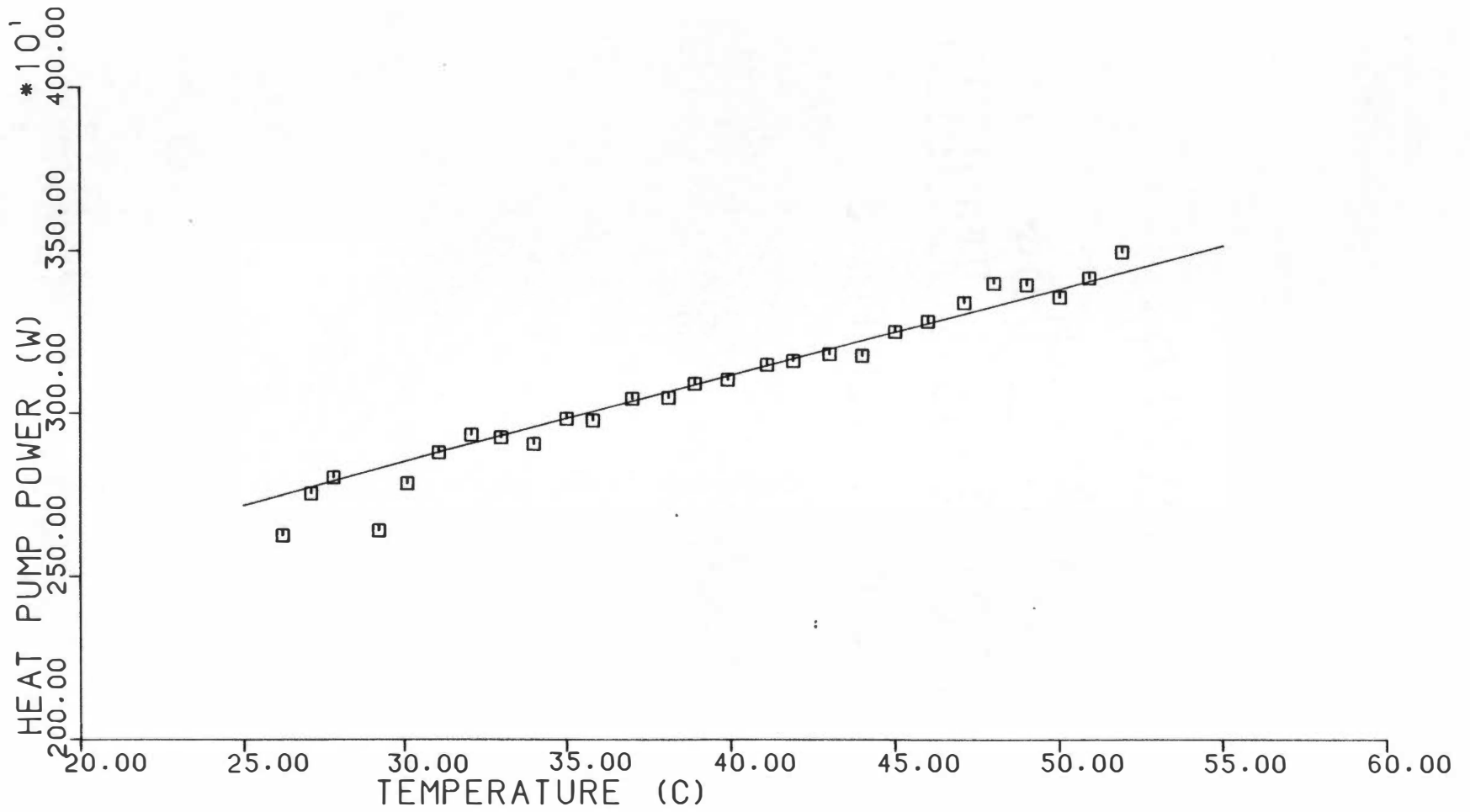


Figure E-3. Temperature vs Heat Pump Power

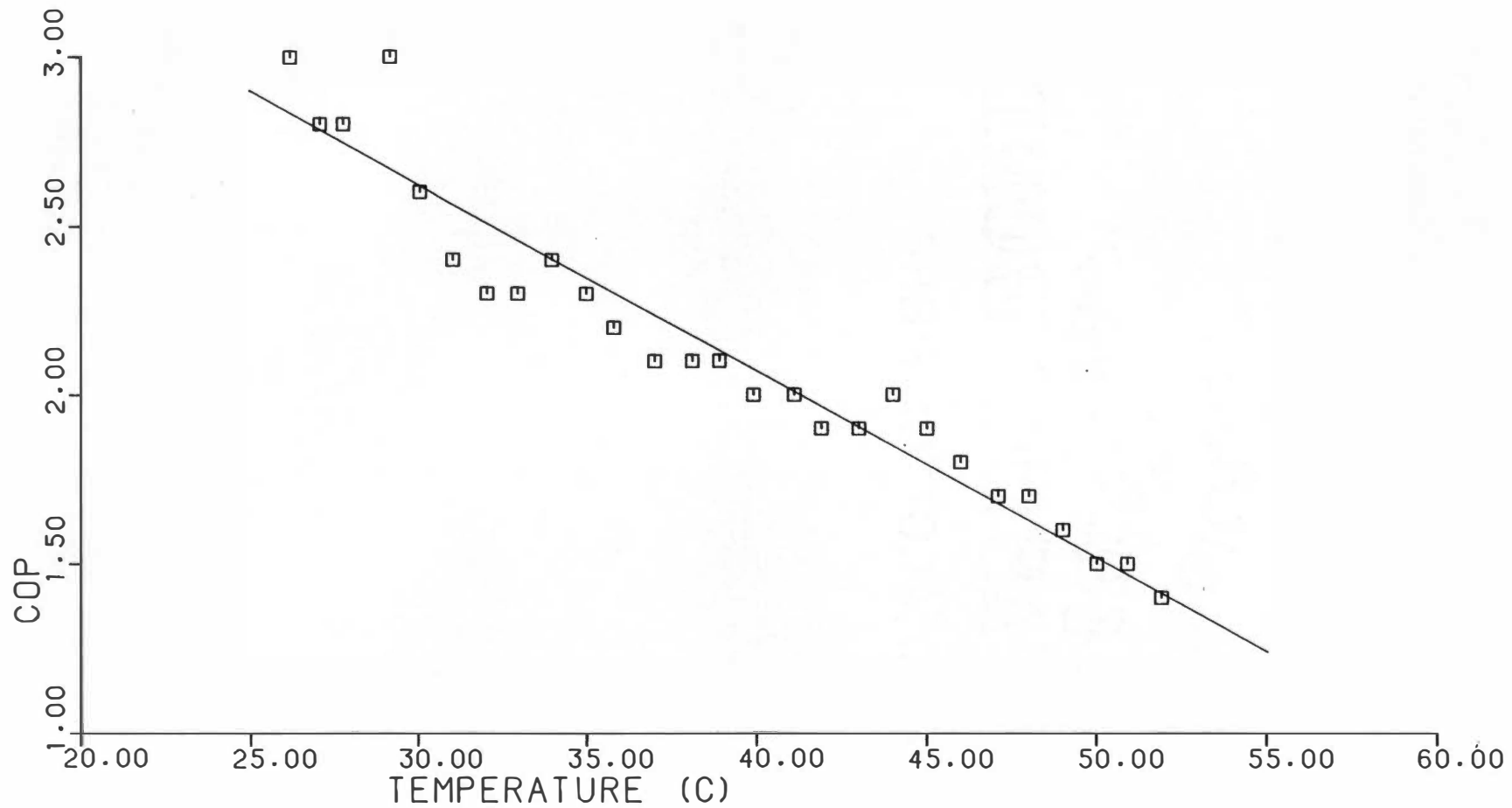


Figure E-4. Temperature vs COP

APPENDIX F

TRNSYS AND GROCS MODIFICATIONS

The TRNSYS TYPE47 subroutine and GROCS were combined to form a subroutine TIPE47. The following modifications were done to TIPE47. It is assumed that the reader is familiar with FORTRAN and has access to the user manuals of TRNSYS and GROCS. TIPE47 contains two sections. The first section is the TYPE47 subroutine and the second section is GROCS.

I. The following array dimensions were increased in order to increase the maximum allowable number of free blocks to fifty. The modified array names and dimensions are listed below.

- A. TSTARF(50)
- B. DEPFRE(50)
- C. VOL(50)
- D. RHOC(50)
- E. DEPRIG(10)
- F. AREA(60,60)
- G. DELTAX(60,60)
- H. QIN(50)
- I. TOLD(60)
- J. TNEW(60)
- K. D(50)
- L. R(60,60)
- M. TSTARR(50)
- N. QNEW(50)
- O. XNEW(50)

II. The variable COND in the GROCS section of TIPE47 was changed to an array to allow individual block thermal conductivities. The array name and dimension are COND(50). The variable COND was replaced by COND(I) in the GROCS section of TIPE47. The input data for GROCS was changed. GROCS requires a description of each block in a certain order as part of the input data. The thermal conductivity of each block was added in a sixth position in the description. The block description and order are:

- (1) The block number
- (2) The initial block temperature
- (3) The depth to the block center
- (4) The block volume
- (5) The block volume heat capacity
- (6) The block thermal conductivity

The read statement used to input the first five factors was modified by adding COND(I).

III. An array CONDOC was defined and contains ten elements. CONDOC allows the user to input individual thermal conductivities to the blocks adjacent to the ground coil. This modification was necessary to make the TYPE47 and GROCS sections of TIPE47 compatible. The adjacent block thermal

conductivities in the TYPE47 and GROCS sections must be the same. CONDOC(I) replaces COND in the TYPE47 section of TIPE47. TYPE47 requires a description of the blocks adjacent to the ground coil. The thermal conductivity of the adjacent blocks was included in the description. The description and order are:

- (1) Block number
- (2) Block length
- (3) Heat transfer area
- (4) Coil to block center distance
- (5) Block thermal conductivity

The following statement was used to input the thermal conductivity:

```
CONDOC(I)=PAR(J+4).
```

This statement follows:

```
X(I)=PAR(J+3).
```

VITA

Steven D. Wix was born in Miami, Florida on September 19, 1955. He attended elementary and secondary schools in Hollywood, Florida and graduated from Miramar High School in 1973. He entered The University of Florida in the fall of 1974 and graduated in 1978 with a Bachelors of Engineering Technology through the department of Mechanical Engineering.

After graduation, he was employed at the University of Florida Solar Energy and Energy Conversion Laboratory for three years. In summer of 1981, he entered the Graduate School of The University of Tennessee, Knoxville and received a Master of Science degree in Mechanical Engineering in June 1984.